Advances in Spectral Optical Code-Division Multiple-Access Communications

Jonathan P. Heritage, *Fellow, IEEE*, and Andrew M. Weiner, *Fellow, IEEE*

(Invited Paper)

***Abstract*—Code-division multiple-access (CDMA) has flourished as a successful wireless networking technology in mobile cellular telephony, and wireless local area networks (LAN) such as the unlicensed industry, science, and medicine (ISM) bands. The commercial exploitation of the benefits of CDMA raises the question as to whether optical code-based communications offer significant benefits to an optical network and what are the technologies that enable code-based optical networks. Recent investigations of optical CDMA (OCDMA) strategies have addressed this question through numerous laboratory-based test-bed studies of multiuser link and recent experimental field trials conducted on in-the-ground fiber. OCDMA requires its own physical layer technologies that are distinctly different from widely pursued wavelength-division-multiplexed (WDM) all-optical networks. Simulations of multiuser performance predict ultimate link capacity and the performance of broadcast and select synchronous nets with strong central management as well as asynchronous architectures with reduced centralized management.**

***Index Terms*—Code-division multiaccess, nonlinear optics, optical communication, optoelectronic devices.**

I. Introduction

INTEREST in the application of code-division multiple-access principles (CDMA) as a potential optical network multiplexing protocol first arose during the late 1980s as the merits of spread spectrum (SS) [1]–[5] for commercial wireless CDMA telephony were being discussed. Wireless CDMA has enjoyed an explosion of applications in the intervening years including the successful deployment of CDMA in cellular telephony networks. CDMA is also used in the global positioning system (GPS) satellite broadcast link. Another major commercial success is the deployment of CDMA in the industry, science, and medicine (ISM) bands, which form the ubiquitous wireless local area networks (LANs) such as the 802.11b that we all use in the workplace and homes to connect our laptops to the Internet.

The commercial exploitation of the benefits of CDMA begs the question as to whether code-based multiplexing offers significant benefits in an optical network. What then are the attributes of CDMA that have made commercial wireless applications so successful and which of these attributes might be exploited by optical networks? Investigations of optical CDMA (OCDMA) in the last two decades have addressed this broad question by proposing, implementing, and demonstrating device architectures to encode and decode a user data stream in the presence of multiple-user interference. Laboratory-based test-bed studies of multiuser point-to-point links using several different OCDMA implementations have been conducted along with performance studies. Recent experimental field trials conducted on in-the-ground fiber have made progress toward demonstrating OCDMA as a useable networking strategy. After reviewing the basic concepts of CDMA in the context of wireless communications, in this paper, we survey important advances in coherent OCDMA, with a specific emphasis on coherent OCDMA achieved via spectral-phase coding.

Manuscript received March 30, 2007; revised May 29, 2007. This work was supported in part by the Defense Advanced Research Projects Agency (DARPA) under Space and Naval Warfare Systems Center (SPAWAR), San Diego, CA Contract N66001-02-1-8937 and Contract N66001-06-1-2028. Any opinions, findings, and conclusions or recommendations expressed in this publication are those of the authors and do not necessarily reflect the views of DARPA and SPAWAR.

J. P. Heritage is with the Department of Electrical and Computer Engineering, University of California Davis, Davis, CA 95616 USA, and also with the Department of Applied Science, University of California Davis, Livermore, CA 94551 USA (e-mail: heritage@ece.ucdavis.edu).

A. M. Weiner is with the Department of Electrical and Computer Engineering, Purdue University, West Lafayette, IN 47907 USA (e-mail: amw@purdue.edu).

Digital Object Identifier 10.1109/JSTQE.2007.901891

II. Multiplexing and CDMA

A. FDM and TDM

Flexible communication systems must manage multiple data streams that access a common transmission link or network of links with finite capacity such as a licensed free-space frequency band, or a physical link such as a coaxial cable or an optical fiber. Multiple streams of data that individually require less bandwidth than the total available bandwidth share the link bandwidth through a multiplexing process. Frequency-division multiplexing (FDM) and time-division multiplexing (TDM) have long been employed in radio as well as optical communications. Systems that utilize FDM assign a unique frequency subband from a number of available subbands, to each user, while, in TDM, each user is assigned a specific time slot from a number of available slots that collectively define a time frame. In large-scale networks, wavelength or time-slot reuse is an important aspect of multiplexing. For example, when transmitters are sufficiently far apart that attenuation renders interference negligible, frequency assignments may be reused. Fiber-optic communication networks typically employ a hybrid of TDM and FDM. FDM is referred to as wavelength-division multiplexing (WDM) in optics. An all-optical network might employ TDM at 10 Gb/s onto a given wavelength band to accommodate many slower users. The fiber can also support many distinct wavelength channels owing to its enormous bandwidth. Wavelength reuse is also possible with WDM networks through separation provided by electronic edge routers or in an all-optical network with wavelength translation.

B. CDMA

Multiplexing is accomplished in CDMA by encoding each user's data stream with a unique logical identifier rather than a time or frequency slot. After encoding, the data stream modulates a carrier, which is transmitted, received, and demodulated along with all other users by each of many receivers. Armed with the knowledge of the codes used by several transmitters, a receiver extracts the desired user from the multitude by comparing the coded multiuser stream with a copy of the desired code and rejecting the codes that do not match.

CDMA, which has its origins in SS system development during and after World War II (WWII), has emerged as an effective multiplexing strategy in certain wireless applications. The term SS is descriptive of the fact that the bandwidth occupied by each user is typically much greater than the bit rate of any single user [6]. The earliest example of the SS technique was based on frequency hopping (FHSS), where an analog or digital signal data stream modulates a carrier frequency, which is shifted in a known, pseudorandom sequence. Each spectral jump is typically much broader than the information bandwidth and during the course of a number of hops, an even wider spectral space is used. Knowledge of the transmitted hopping pattern by the desired receiver allows reconstruction of the signal stream provided a method to synchronize a receiver's spectral passband time hopping is provided. FHSS systems are relatively immune from narrow band jamming by virtue of the fact that little time is spent at any one frequency. The pseudorandom hopping also provides a measure of obscurity to eavesdropping with conventional receivers.

C. Direct Sequence SS (DSSS) and Codes

Wireless CDMA systems today frequently employ DSSS as a multiplexing strategy. In DSSS, each information bit is modulated with a temporal code sequence that changes state rapidly compared to the information bit length. As depicted in Fig. 1, each information bit is encoded through rapid temporal modulation by a binary phase code, although multilevel codes are possible. Colloquially, one says that each bit is chopped into a large number of "chips" by temporal modulation. For purely phase-based codes, the encoded bit remains unchanged in temporal profile but the spectrum is spread by the temporal modulation into a much broader noise-like spectral signature as suggested by Fig. 1(a). In a communications system, multiple users are each assigned a unique code and each user bit stream modulates a common carrier, which is broadcast. The receiver demodulates the carrier, which results in a baseband signal, which is a superposition of all of the various bit streams. Each receiver then decodes its desired coded sequence from the superposition by multiplying the incoming mixture of sequences with a conjugate of the desired code sequence. For the case where synchronism has been established between the conjugate code and the desired user's code the resulting signal from the desired user is *spectrally despread* to its original bandwidth. If the undesired channels are also synchronous, then orthogonal codes may be employed and the interfering user signals remain spectrally spread. The output of a bandpass filter with bandwidth set wide

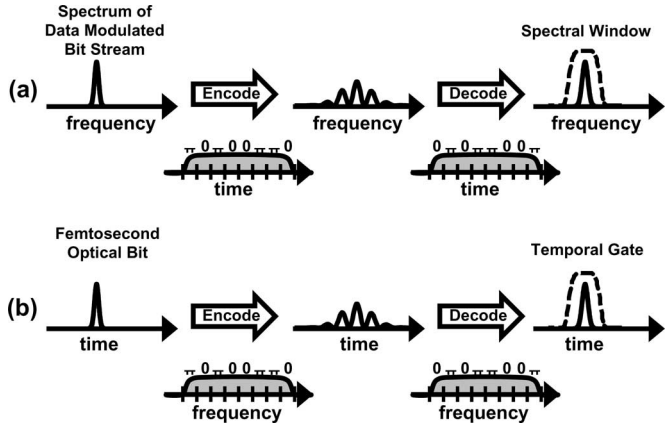

Fig. 1. Schematic representation of (a) direct sequence SS and (b) its dual, spectral-phase modulation, for CDMA and OCDMA, respectively. Only correctly decoded user is depicted. Other users remain spread either in frequency or time and are rejected by the spectral filter and its dual, the temporal gate.

enough to pass the despread signal but narrow enough to reject most of the spread signals is sampled by a threshholding circuit. For a large spreading ratio, the contrast between the correct user's signal and the sum of the interfering users is large, and the desired signal may be detected with a high signal-to-noise ratio.

A desirable family of codes has the property of orthogonality, whereby multiplication of any two different *temporally aligned* members yields another sequence that sums to zero, which implies that the bit's spectrum remains spread and that there is a zero signal within the passband of the receiver's low-pass filter. Binary orthogonal codes are constructed to take advantage of the phase difference of 0 and π, or equivalently 1 and -1 in signal amplitude, to build families of sequences whose cross correlations sum to zero. The families of Walsh–Hadamard codes are examples of orthogonal code sets. The orthogonality property of these codes allows a number of users, each assigned its own code member of the orthogonal code family can simultaneously use the network without interfering with other users. Implementing a purely orthogonal coding scheme requires the strict implementation of the mathematical cross-correlation properties. This can be done in only certain ideal cases where *phase coherent demodulation* can be assured and precision *temporal overlap* among all users be firmly established. In general these are difficult conditions to assure; in this case, pseudoorthogonal codes would be chosen that maintain relatively low cross correlations for imperfect temporal overlap.

D. CDMA in Cellular Wireless Telephony

One example where the use of orthogonal codes is possible and is effectively deployed is for the base-station to mobile-station link in CDMA-based wireless cellular telephony [7]. The cell base station broadcasts a number of uniquely encoded channels that have been temporally aligned on a common, stable, low-phase-noise carrier. Each mobile receiver employs a phase-lock loop to demodulate the carrier producing a signal composed of a superposition of all the simultaneous user's codes, each with

amplitudes of 1 and -1 preserved. After establishing synchronism of the local complimentary code with the multiuser signal, the desired user signal can then be extracted by performing a cross-correlation with the complimentary code. This is the ideal situation where the desired user can be selected in the presence of other users as if there were no other users present. In this case, spectral efficiency will be at its highest and system capacity will be at its maximum, if we set aside, for the moment, the impact of multipath interference.

When either/or both coherent detection and temporal alignment is/are not feasible to implement, then orthogonality is lost and there will be potentially substantial multiuser interference (MUI) that can seriously degrade the system performance. MUI is partially mitigated by the use of *pseudoorthogonal* codes. For a code of length N, where N is the number of chips, the autocorrelation at zero delay is equal to N. In comparison, pseudoorthogonal codes should have cross correlations between two temporally offset codes that are nonzero but less (hopefully much less) than N, for all time delays. The value of the cross correlation, for zero-time offset, is typically no longer zero as well.

For existing cellular systems, the return link is not synchronous and the carrier phase of various channels remain uncorrelated. The result is the return link would have much poorer BER performance than the uplink owing to the onset of coherent interference Fortunately, for narrow-bandwidth systems adequate for intelligible voice, a BER of only 10^{-3} is required and error correction (FEC) [8], [9] to achieve even this modest reasonable BER performance is required. In addition, the multitude of low-cost oscillators in each mobile station must be locked to a pilot tone transmitted by the base station. Interestingly, both a local feedback loop is used as well as a loop, which includes feedback from the cell base station as it attempts to optimize the BER of each return link.

E. Benefits of Wireless CDMA

What are the most significant benefits to the use of CDMA wireless systems? For wireless CDMA-based telephony, the principal benefit is in spectral reuse [10]. This point is illustrated by considering a simple two-dimensional array of close-packed hexagons of equal size with the base station at each cell center, a simplified model of a cellular topology. Each hexagonal cell is surrounded by six such hexagons. In FDM cellular, each cell must not share frequency allocation with each of its six nearest neighbors because frequency channels are separated by broadcast attenuation only. Thus, in this simplified example, each FDM cell can use only 1/7 of the frequencies available in the licensed band; furthermore, the frequency assignments are allocated in advance and are fixed. In CDMA, no such frequency allocation assignment need be made and a single (software programmable) transmitter/receiver suffices. Each cell has at its disposal all codes to assign to users as traffic demands and as necessary to not interfere with adjacent cells. Furthermore, dynamic code assignment is handled in software; provisioning of multiple fixed transmitters is not needed as in FDM or TDM systems.

The point of our discussion about wireless CDMA is to obtain some level of appreciation of the complexity required to implement a CDMA system and the benefits that accrue. This discussion illustrates important tradeoffs. In particular, efficient spectral use requires extensive management, control, and signal processing complexity. In contrast, systems may implement simplified management and control but at the cost of much lower spectral efficiency, resulting in greatly reduced number of simultaneous users due to unavoidable multiuser and coherent interference.

There are many other aspects of wireless CDMA that are important, including multipath interference and the use of the so-called RAKE receiver, which can resynchronize delayed images of the desired signal and thereby eliminate coherent interference. The RAKE receiver also enables "soft" (make before break) handoffs as a mobile station crosses cell boundaries by simultaneously receiving identical coded data streams from adjacent cell master stations! In addition, the near–far problem, where strong signals swamp the reception of weaker signals in an asynchronous system, is especially important. In fact, in cellular telephony, the base station must control the transmitted power of each and every mobile station in order to assure nearly equal power received from each transmitter so that more remote terminals are not dropped.

III. CDMA TO OCDMA

The proposed use of direct sequence modulation SS as a basis for wireless commercial CDMA telephony emerged in the 1980s and numerous claimed advantages of CDMA over TDMA prompted interest by some [11], [12] in a search for methods to transfer CDMA principles, and presumably, benefits, into optical networks. It was not evident, *prima facie*, which benefits would transfer to fiber-optic-based communications. Also, it was not immediately evident how to effectively implement the OCDMA. Optical communication networks are quite different from the commercially successful wireless CDMA systems in several crucial ways. Wireless systems typically are low bit rate ($\sim$10 Kb/s for cellular), are tolerant of relatively high bit-error rates (BERs) ($\sim 10^{-3}$), and typically involve mobile stations. Most significantly, the low bit rates allow wireless systems to enjoy the considerable benefit of Moore's law that has delivered rapid growth in electronic signal processing power while decreasing cost and size over the last two decades. Thus, it has been both cost effective and technically feasible to implement wireless communications systems, such as cellular telephony, that require extensive system management as well as local processing power to enable forward error correction (FEC), for example, and thus assure adequate performance for the user and cost effective management for the service provider.

In contrast to wireless, fiber-optic-based communications systems enjoy access to enormous fiber bandwidth and immunity to external interference sources, are free of multipath interference, and are not mobile (although they might very well need to be rapidly reconfigurable). Furthermore, switched WDM networks deliver scores of very high-speed (>10 Gb/s) links using only a few fibers that span continents. In short, CDMA has been especially effective in solving problems for wireless networks

that at first glance do not appear to be problems at all in optical networks.

Nonetheless, the list of potential advantages of code-based multiplexing in optical communications is attractive. The list includes: 1) flexible access to wide bandwidth, 2) code-based dynamic reconfiguration, 3) decentralized networking, 4) passive code translation, and 5) a measure of security through data obscurity. These benefits would enable one to construct an "all-optical" LAN where O-E-O conversion would not be required for routing or circuit switching as commonly employed in WDM systems.

The benefit of a commercially successful all-optical OCDMA network would be a flexible network with a simplified access protocol, essentially locally managed, and with potentially asynchronous access. To the network provider would accrue the benefits of reduced central management requirements, and the flexibility to deliver bandwidth on demand or other quality of service (QOS) requirements through software (code)-based management without the need to provision each user with frequently unused hardware. Research in OCDMA has attempted to address these issues in the last two decades by exploring how OCDMA might be implemented and how that implementation performs. Much has been accomplished in investigating what unique hardware is required to realize a particular implementation, how to build test beds to explore performance in a laboratory environment, to invent, fabricate, and test potentially new optical and optoelectronic OCDMA-enabling devices. In addition, field trials have been conducted in realistic in-the-ground fiber-optic links.

IV. Early OCDMA Investigations

In 1986, Prucnal [13] provided the earliest experimental demonstration of an attempt to migrate DSSS-like CDMA concepts into the optical domain using a single-fiber communication link. Fiber delay lines construct an encoded temporal sequence of optical chips, called prime codes, which represent a bit of information. Each binary chip is indicated by the absence or presence of optical energy. Prescribed sequences of chips form a bit of information. The decoder is a set of complimentary optical fiber delays arranged to recombine all of the energy into a single pulse that is detected with a sufficiently fast square-law photodetector. Unfortunately, successful rejection of other users requires codes with a preponderance of zero-energy chips thus limiting channel bit rate. Salehi [14], [15] explored the performance of a CDMA link using energy-based "optical orthogonal codes," in a multiuser link and found that energy-based codes must be sparsely populated to obtain reasonable link capacity.

Salehi's results led the authors of this paper to consider ways to implement binary phase codes in the optical domain in a method that retains the advantage of phase cancellation enjoyed by DSSS CDMA, yet would readily scale to very high user bit rates in anticipation of the inevitable move toward today's 10–40-Gb/s optical link capacity. Encoding in our scheme is accomplished by impressing phase codes on the *spectral field* of ultrashort optical pulses, rather than attempting to encode an ultrashort optical pulse in the time domain.

A CDMA system employs one of the several possible multiplexing schemes where data streams are encoded with a random signal. We were well positioned to demonstrate this idea at the time using our femtosecond pulse shaping technique [16], [17] which we had recently invented, analyzed [18], and demonstrated [19] with 100-fs optical pulses. The pulse shaper, which is described in more detail in Section V, uses a pair of gratings and lenses to map optical frequency into space. In this manner, a spatial optical phase mask imposes a bipolar phase sequence on the *spectrum* of the ultrashort pulse. This approach, as depicted in Fig. 1(b), is the dual to DSSS CDMA. Encoding in the spectral domain results in the *spreading* of the ultrashort pulse in the *time domain*, in close analogy to the way *temporal* modulation produces a *SS* in DSSS. The resulting noise-like temporal pulse is transmitted to a receiver, which consists of a pulse shaper decoder. After decoding, the phase of the resulting spectrum is frequency invariant, which means that the noisy pulse is temporally *despread* back to the original pulse shape just as the spectrum of a correctly decoded DSSS-modulated pulse despreads to its original bandwidth. When another user injects a spread pulse into the link using a different member of the chosen code set, the decoder phase spectrum is such that it does *not* despread the pulse. Encoding and decoding of the spectral phase of a pulse was demonstrated for the first time by Weiner *et al.* in 1988 [20].

The optical detector, which is placed after the decoder, must be capable of distinguishing between the despread pulse and the sum of all of the remaining spread pulses. For systems where the despread pulse is in the picoseconds time-scale or less, even the fastest photodetectors cannot distinguish between spread and despread pulses. Optical signal processing based on high-speed nonlinearities is required. Examples of high-speed optical devices that potentially provide the desired discrimination include harmonic generation with second-order optical nonlinearities, and fast temporal gates or wavelength conversion, which both use fast third-order nonlinear interactions in fibers. Each of these techniques is discussed in Section VIII.

The initial measurements in [20] clearly demonstrated the principles of temporal spreading and despreading, but their use in a demonstration communications link had not yet been shown. In order to assess the potential of spectral OCDMA and temporal spreading/despreading, Salehi *et al.* [21] analyzed the BER performance of an ideal spectral OCDMA link with multiple users. The structure of the basic spectral OCDMA link analyzed in [21] is depicted in Fig. 2. The link comprised of an ultrashort pulse mode-locked laser source, a grating and lens spectral-phase encoder, an ideal dispersion-free fiber link on to which multiple users are added in an M $\times$ M star coupler, and an idealized high-speed thresholding device. The spatial resolution of the pulse shaper and multielement phase modulator was assumed adequate to support codes with N_0 chips. Code lengths of up to 512 spectral chips were considered. The receiver consisted of a matching grating and lens spectral-phase decoder and an ideal fast detector. The simulations assumed that optical interference due to multiple uncoordinated users is the key factor determining performance. Such interference includes both those portions of the interfering users overlapped in time with a

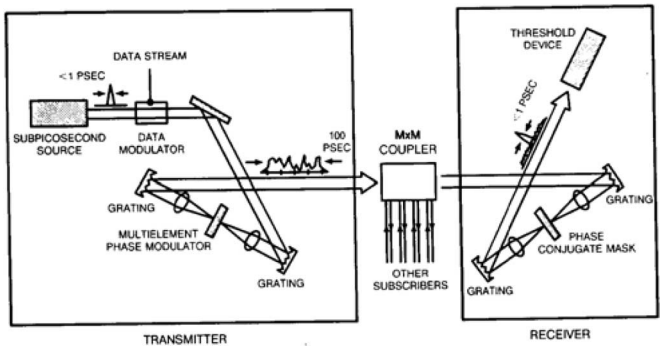

Fig. 2. Spectral OCDMA transmitter with encoder, added subscribers, and receiver with conjugate decoder. (Salehi *et al*. [21])

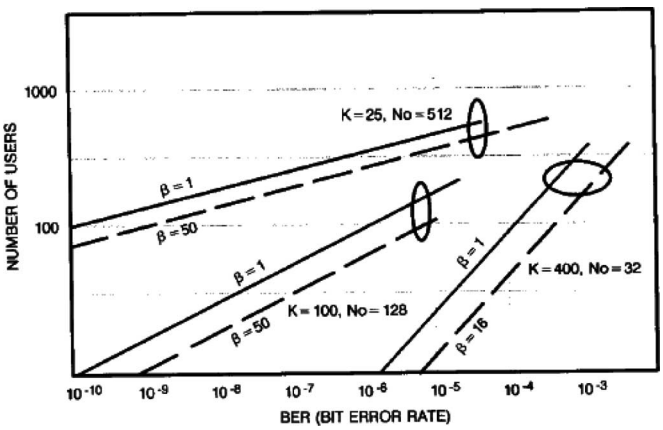

Fig. 3. Calculated number of potential users against the BER. Parameters are defined in text. (Salehi *et al*. [21])

decoded short pulse signal and those portions not overlapped in time. In [21], both forms of interference are designated multiaccess interference (MAI). A more recent theory [22] specialized to a different OCDMA implementation based on time-domain phase encoding, uses the term MAI to denote only the nontemporally overlapped interference and introduces a new term, signal-interference beat noise (SI) to denote the temporally overlapped interference. Nevertheless, both theories fully account for both types of interference. The temporally overlapped interference, or signal-interference beat noise, is generally the more serious interference term. In this paper we generally use the term "multiaccess interference" or "multiuser interference" to refer to both types of interference.

A time-slotted link was assumed where each of the N users was randomly assigned to one of the K uniform slots, which are just long enough to accommodate the spread optical pulse. The results of Salehi's simulations are summarized in Fig. 3 where the number of users that can be supported at a particular BER is plotted as a function of the BER required. Since the period is proportional to the number of time slots, K, multiplied by the spreading ratio, N_0, the results are plotted for the constant product $KN_0 = 12800$. This means that each of the curve families are for the same user bit rate, which is equal to or less than $1/KN_0\tau_c$, where τ_c is the source laser pulse width. For example, if $\tau_c = 80$ fs, then the greatest single user bit rate is 1 Gb/s. We see that long codes and fewer time slots are more effective at allowing more users and, thus, are more effective at suppressing multiuser interference than short codes and greater number of time slots. The parameter β is a measure of the speed of the thresholder. For $\beta = 1$, the thresholder response time is treated as equal to τ_c and, for $\beta = 50$, the thresholder response time is 50 times longer. Calculations, which included multiuser interference, show that long code lengths (large temporal spreading ratios) are most effective in overcoming multiuser interference and that with slotting, a large number of users is possible. Conversely, calculations suggested that short code lengths are rather poor at suppressing MUI as evidenced by the curves for $K = 400$ slots and code lengths of only 32 chips. In that case, even with a collision probability of only 1/40, ten users would suffer BER of $\sim 10^{-6}$, which means there is an expectation of severe MUI when coded pulses happen to overlap in time! In [23], the authors established a simple upper-bound calculation to the expected BER performance and included performance calculations for $K = 1$ and an enormous code length of $N_0 = 12800$.

At the time of these papers, no link BER performance measurements had yet been made for experimental comparison, even for a single user. Nonetheless, these calculations showed that coherent spectral OCDMA was a promising path for moving from low-bit-rate wireless DSSS concepts to the optical domain where superbroadband optical pulses and high bitrates make spectral modulation and time spreading a natural mode of operation.

It should be noted that phase encoding and decoding in the optical spectral domain is but one of two broad strategies toward coherent OCDMA. Coherent phase encoding and decoding has also been performed successfully using passive tapped delay line (transversal filter) structures. A recent theoretical study [22] of coherent OCDMA in such a time-domain coding architecture confirms the importance of long code lengths in minimizing interference and indicates the need for additional strategies such as synchronous gating to minimize the severity of interference as a link impairment. Such additional strategies are also quite relevant for coherent OCDMA based on spectral encoding and decoding.

Another OCDMA approach that has subsequently been explored in efforts to overcome the severe inefficiency of the original energy-based optical codes, employs both time and wavelength space to form two-dimensional (wavelength and time) energy-based (incoherent) codes, thereby enabling greatly expanded code lengths and increased flexibility in code design. This approach is reminiscent of frequency hopping SS in the RF domain. Two-D code chips are still represented by the presence or absence of energy, but now both in time and wavelength. We will not pursue the incoherent 2-D code approach in this paper as it is addressed in detail elsewhere in the special issue.

V. Free-Space Optics Spectral Encoder/Decoder

Coherent spectral encoding and decoding for OCDMA, as was first introduced in [20] uses the bulk optic femtosecond pulse shaping technique [16]–[19]. A recent review of free-space

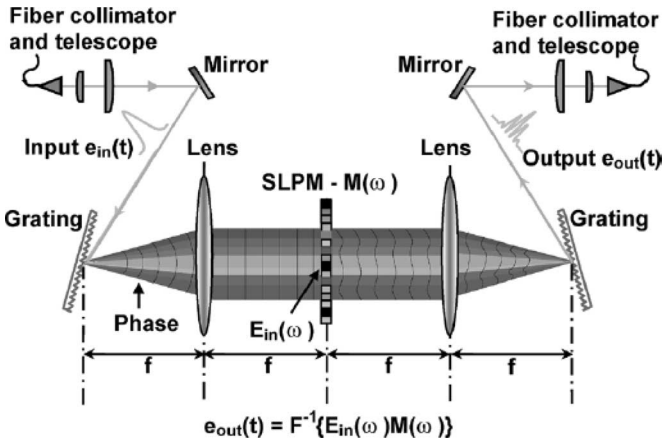

Fig. 4. Femtosecond pulse shaper used as a spectral encoder or decoder. The focal length of each lens is f. The spatial light phase modulator (SLPM) maps a prescribed spatial phase-shift pattern onto the pulse spectrum.

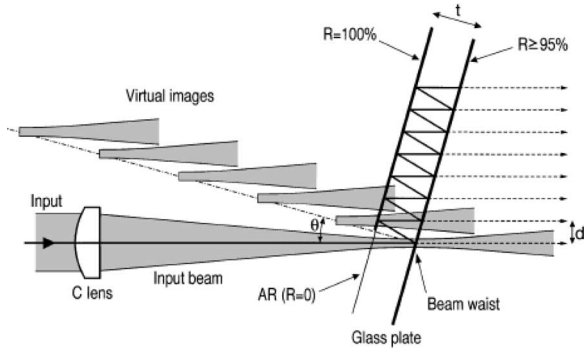

Fig. 5. VIPA. (Shirasaki [27])

pulse shaping, emphasizing programmable implementations is given in [24]. Fig. 4 illustrates how spectral-phase modulation is impressed on the ultrashort pulse using the grating and lens femtosecond pulse shaper. Two such devices were used in an OCDMA communication link; one located at the transmitter encodes while a second located at the receiver decodes.

The pulse shaper consists of two coaxially located lenses spaced to share a common focal plane. Antiparallel gratings are placed precisely in each of the other two lens' focal planes. A spatially patterned, electronically addressable, phase and/or amplitude spatial light modulator (SLM) is located precisely in the focal plane common to the two lenses. Each optical frequency component of the spectrum of an input pulse or modulated pulse train is focused to a small spot size at its unique spatial location on the SLM and is reconstructed spatially into a single pulse at the output. The temporally reconstructed pulse is, in the absence of an imposed spatially varying phase by the SLM, identical to the input as the paths are dispersion-free. If, on the other hand, a spatial phase variation is imposed by the SLM on the spectrum, then the output pulse's temporal electric field profile is given by the Fourier transform of the input electric field amplitude as modified by the amplitude and phase spectrum contributed by the SLM.

This picture is valid to a good approximation for high-resolution configurations where the spot size on the SLM is much smaller than the spatial spread of the spectrum as set by the grating dispersion, spot size on the grating, and focal length of the lens. The resolution of the encoder is defined as the ratio of the optical spot size at the focal plane to the total spatial spectral spread at that focal plane. In general, higher resolution is obtained with larger beam diameter on the grating, greater grating spectral dispersion, and greater input pulse spectral bandwidth. Intuitively, high-resolution situations are characterized when the spectrum appears as a broad, sharply focused line at the focal plane of the lens. Practical encoder resolution can be as large as several hundred, or more, at 1.55-μm wavelength for carefully optimized designs and optical pulse widths $\sim$100 fs. The resolution plays an important role in system design as it determines how long a code (number of chips) can be impressed on a pulse spectrum provided an efficient spatial light modulator can be constructed with a large number of tiny addressable pixels. Presently, typical addressable SLMs commercially available provide 128–256 pixels, suitable for code lengths of 64–128.

For longer input pulses corresponding to reduced bandwidth (consider, for example, the bandwidth of a typical WDM channel), the maximum number of chips that can be employed may be severely constrained by the resolution. A relative of the grating and lens encoder that has been used to provide improved resolution in spectral OCDMA demonstrations [25], [26] uses a virtually imaged phase array (VIPA) [27]–[29] as a spectral disperser, in place of a grating. The VIPA is a modified Fabry–Perot interferometer illuminated by a focused line source incident at an angle and injected into the Fabry–Perot through an uncoated or antireflection-coated window. As depicted in Fig. 5, spatial walk-off of multiple reflections are equivalent to a virtual array of line sources, which form a virtual grating. When combined with a Fourier lens, the pair behaves as the grating and lens device described earlier. VIPAs can be designed to have high spectral resolution because they can be made equivalent to a short-pitch grating, which enables separation of individual axial modes of data streams at $\sim$gigaherz rates over a limited spectral range. In addition to spectral encoding and decoding, VIPA-based pulse shapers have also been demonstrated for other optical signal processing applications such as programmable dispersion compensation at high spectral resolution [30]. Grating-based devices appear to be most appropriate for use with ultrashort pulses and high repetition rates while the VIPA is useful for reduced optical bandwidths where its high resolution enables precise phase modulation of a handful of individual spectral components.

VI. Guided-Wave Spectral Encoders/Decoders

While the free-space optical encoders are excellent devices useful for laboratory test-beds built on optical tables, a practical OCDMA system requires guided-wave devices for their compact size, potential for large-scale integration, ease of use, and potential low costs in a high-volume market. Research in developing planar waveguide circuits and structures fabricated in silica or InP for OCDMA has progressed in the form of passive silica arrayed waveguide gratings (AWGs), integration of

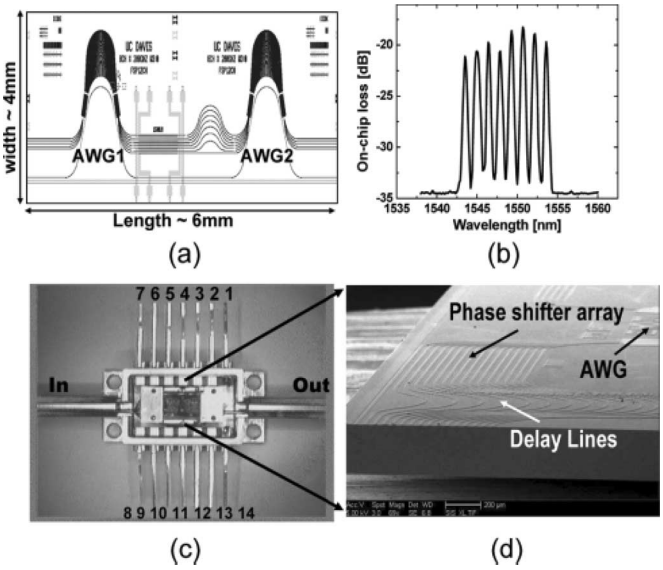

Fig. 6. Planar integrated circuit encoder/decoder. (a) OCDMA encoder chip layout. (b) Transmission spectrum. (c) Packaged encoder. (d) Scanning electron microscope (SEM image). (Cao *et al*. [33])

passive and active devices in InP, fiber Bragg gratings (FBGs), and ring resonator circuits.

A. AWGs and Integration

AWGs fabricated in silica and InP been developed for spectral OCDMA. In 1999, Tsuda *et al*. [31] reported spectral-phase encoding and decoding of a 10-Gb/s ultrashort pulse train (despread pulse width ~800 fs) using a high-resolution reflection-mode silica AWG as an encoder/decoder and a 255-chip spatial phase filter consisting of a patterned Au mirror. Fiber pigtailed circulators separated the encoded returned signal from the input. The detector was a conventional receiver (no ultrafast thresholder was used) and, thus, only single-user performance was reported. Nonetheless, the measured BERs for a single user as a function of power showed that error-free performance could be achieved in the absence of MUI.

The development of a fully integrated OCDMA transceiver including laser source, AWG encoders/decoders, and nonlinear optical signal processing is a major challenge that would enable cost-effective, compact OCDMA transmitters and receivers. Broeke *et al*. [32] reported progress toward integration in the form of an inline InP-based encoder/decoder with integrated phase modulators. Fig. 6 shows a sketch of their waveguide-based encoder. AWG1 is designed to separate the spectral components into a number of planar waveguide output arms. Each output arm is fabricated with a waveguide electrooptic phase modulator. High-speed phase modulators may be designed and fabricated in InP giving an encoder/decoder the capability of changing the code ultimately on a bit-to-bit basis. AWG2 recombines the encoded spectral components. The AWGs were designed with a process flow that is compatible among the many different devices that need to be fabricated on a single chip [34]. This group has also demonstrated progress toward development of lasers that can also be integrated [35] in a common process flow as well as a Mach–Zehender wavelength converter that would serve as the foundation of an integrated nonlinear optical thresholding device [36]. Such integrated chip solutions, when sufficiently developed and successfully refined, would significantly contribute to further progress in OCDMA.

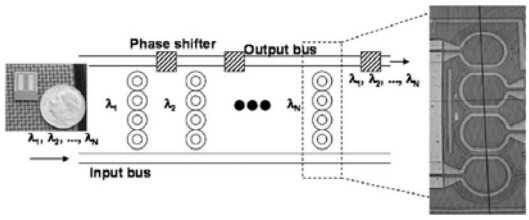

Fig. 7 Integrated ring resonator spectral-phase encoder schematic and SEM micrograph of overlaying heater structure. (Agrawal *et al*. [37])

B. Microring Resonators

Microring resonators fabricated from high refractive index glass in planar waveguide geometry are arranged in a bus structure, as depicted in Fig. 7 [37]. These devices form a spectral-phase coder. A common input bus and a common output bus are combined with stacks of microring resonators that form a fourth-order resonator. Each stack acts as a bandpass filter between the two buses, as shown in Fig. 7. Each passband defines frequency bins, which, in the present case, have a 3-dB bandwidth of 8 GHz with a channel spacing of 10 GHz. A number of microring resonator stacks are tuned to select individual axial modes of a mode-locked laser and the associated sidebands resulting from data modulation. The resonator rings are fabricated in a plane above the plane of the buses separated by a thin deposition layer with precisely controllable thickness. The device used included eight bins spaced on a 10-GHz frequency grid. The relative phase shift between two adjacent frequency bins is controlled by thermooptic phase heaters along the buses and this phase shift can be continuously varied between 0 and π on a millisecond time-scale. The individual ring resonators are temperature tuned as well. This device is well suited for high-resolution spectral encoding over finite bandwidths and has been successfully used in test-bed experiments at Telcordia. These results are discussed in Section IX-B.

VII. Time-Spreading OCDMA—FBG

Another technique used in coherent OCDMA is time-spreading OCDMA (TS-OCDMA) [38] where short optical pulses are directly spread through the use of devices that map time to space. This is analogous to pulse shapers, which map frequency to space. Recent spectacular results have been presented using FBGs that allow the implementation of very long spectral codes and have produced world-record-class link capacity in a truly asynchronous demonstration [39]. One of the devices typically employed in TS-OCDMA is the superstructured FBG (SSFBG) [40]–[42]. Although many types of SSFBG have been described in the literature [43], the type typically used in TS-OCDMA is essentially a series of FBGs, as shown in Fig. 8˜. Each of the individual FBGs has a common grating

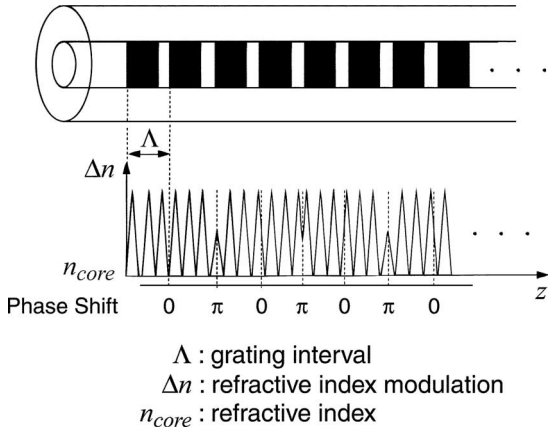

Fig. 8. Structure of the phase-shifted SSFBG. (Hamanaka *et al*. [39])

period, length (i.e., interval, Λ), refractive index modulation, Δn, and a possible phase shift at the grating intervals. As a short optical pulse propagates through the SSFBG, it generates a reflected response that consists of a series of "chip" pulses. The relative phase between the chip pulses is determined by the pattern of phase shifts in the SSFBG. Generally, fabrication is accomplished using holographic techniques. Although individual devices have fixed codes, a key advantage of SSFBGs is that they provide the longest code lengths to date in OCDMA [44].

VIII. Nonlinear Optical Signal Processing

After the information bit is despread by the decoder, a signal must be identified and retrieved. The retrieval involves rejection of multitude of spread user bit streams. On the other hand, the desired despread user's optical pulse stream must be converted into to an electronic bit stream that reproduces the desired user's bitstream with low-error probability. The challenge is that in the spectral encoding approach, each of the interfering spread pulses contains as much energy as the desired despread pulse. If electronic processing were fast enough, then high-speed electronic detection and thresholding circuits would be able to distinguish between the despread pulse and the superposition of a number of spread pulses. In an all-optical OCDMA network, we wish to transmit data at a high bit rate, for example, 10 Gb/s. A spreading factor of at least 100 would be desirable to support a useful number of simultaneous users. Then, the detector and thresholding electronics must have a response time $\sim<1$ ps or better in order for the circuit to be able to distinguish between the high-intensity despread pulse and low-intensity spread pulses each of which contains as much energy as the despread pulse. While terahertz electronics might be on the horizon, they are not readily available today and were unthinkable in the 1980s when the first demonstrations of the concept were presented. Nonlinear optical signal processing, which can be as fast or faster then the despread optical pulses, has been the solution to this problem. Unfortunately, nonlinear optical effects typically require relatively high input power and long interaction lengths in order to provide useful effects. Progress toward OCDMA nonlinear processing devices with high nonlinear sensitivity is discussed further in Section VIII-B.

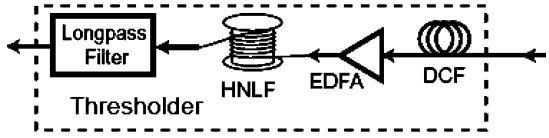

Fig. 9 Intensity discriminator including dispersion-compensated amplification (DCF and EDFA), nonlinear fiber, and long-pass filter. (Sardesi *et al*. [45])

The receiver must distinguish between a despread ultrashort pulse when the desired transmission is decoded, and a time-spread, noise-like superposition of spread pulses, each with the same energy. Several nonlinear optical methods have been employed to accomplish this important task. They include self-phase modulation in fibers, second-harmonic generation (SHG) in periodically poled lithium niobate (PPLN), and synchronized optical gating using a nonlinear optical loop mirror (NOLM).

A. Nonlinear Spectral Broadening in Fiber

Early experimental spectral OCDMA proposals demonstrated the idea of using time spreading and despreading with visible wavelength mode-locked lasers and standard femtosecond optical cross-correlation techniques to explicitly measure temporal intensity profile of spread and despread pulses. The first optical thresholding device capable of distinguishing between spread and despread pulses with sensitivity adequate for demonstrating OCDMA principles was introduced in [45] by Sardesai *et al*. This reference made use of the long interaction length possible in a dispersion-shifted fiber (DSF) for efficient nonlinear generation of spectral broadening coupled with spectral filtering to obtain effective intensity discrimination. Fig. 9 is a schematic of a generic thresholder. Despread pulses are of much higher intensity than spread pulses and, thus, the generated spectral broadening arises predominantly from the despread pulse while the spread pulses contribute little to this process. A long-pass filter placed at the DSF fiber output transmits these broadened components that are passed through to a conventional communications receiver. Fig. 10 shows the measured broadened spectra generated by a properly decoded optical pulse, in the presence of three interfering users as reported by Scott *et al*. [46]. Also shown is the spectrum generated by the three interfering users alone. The correctly decoded pulse is passed by the long-pass filter while interfering users are rejected. In this example, the authors of [46] replaced the DSF fiber of the early work with a highly nonlinear fiber (HNLF) and were able to achieve improved sensitivity.

B. Quasi-Phase-Matched Harmonic Generation

One solution to the need for a robust power budget for an OCDMA system with a large number of users is to find a means to substantially increase the sensitivity of the nonlinear detection method employed to distinguish between the spread and despread optical pulses. Zheng *et al*. [47] introduced a long, PPLN SHG waveguide [48] as a promising, high-sensitivity, optical nonlinear device for spectral OCDMA. The use of a

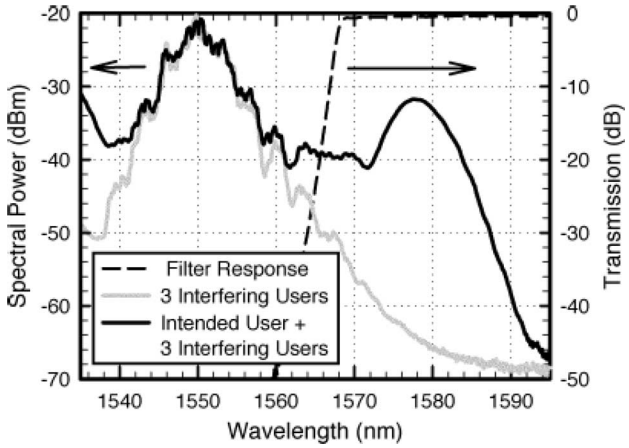

Fig. 10 Spectral plot demostrating how the thresholder discriminates between intended user and interfering user's signals. The high peak power of the intended user's pulses generate additional spectrum (black trace) when compared to the spectrum from interfering users (gray trace). Spectra greater than 1568 nm are selected by the longpass filter (dashed trace).

waveguide structure together with a long, quasi-phase-matched nonlinear medium leads to dramatically improved detection efficiency compared to bulk SHG and a significant improvement over fiber nonlinear interactions. Their results enabled real-time all-optical recognition of spectrally phase-coded optical pulses at subpicojoule pulse energy levels [47]. Thresholders based on nonlinear frequency shifts in DSF require much higher pulse energy levels of ~25 pJ [45], while the use of a HNLF fiber threshholder in place of the DSF reduced the required energy to ~15 pJ [49]. PPLN thresholders have been successfully used in multuser link demonstrations that required the least pulse energy to achieve excellent BER yet reported. These advances are discussed in Section IX.

C. Synchronous Gating of Despread Optical Pulses

A nonlinear thresholder, such as the frequency shifting fiber and SHG architectures described earlier requires no special precision clock for timing. However, fluctuations arising from coherent interference among all of the time-spread incorrectly decoded users are strong. Interference between despread pulse and the portion of the spread pulses that coincides with the despread pulse also grows as the number of users increases. The total optical power, which is carrier-phase- and envelope-delay dependent, is proportional to the square of the sum of all real optical fields. If no effort is made to guarantee full phase synchronization among all users at each receiver's location, a challenging task that has not yet been accomplished, then system performance is severely affected. This interference effect, which may be thought of as a temporal analog of optical speckle, is the fundamental challenge that must be solved if one requires the highest possible spectral efficiency in OCDMA. It is relatively straightforward to assure full coherence only in very special system architectures. In wireless telephony, the base-station-to-mobile-receiver broadcast link, as discussed in Section II-D, is one such example where coherent detection is assured through phase-locked detection of a single radio frequency (RF) carrier supporting multiple data streams.

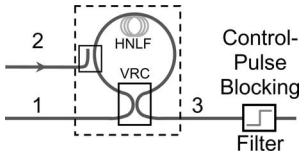

Fig. 11. Fiber-optic NOLM gate. HNLF-higly nonlinear fiber, VRC-variable ratio coupler.

Interference among the numerous incorrectly decoded optical data pulses that extend well beyond the despread pulse width may be suppressed with a temporal gate. Of course, the gate must be fast; it must open and close rapidly around the despread pulse and the time of the gate opening must be precisely synchronized with the arrival time of the despread user. Once the decision to synchronize the gate with the despread pulse is taken, another strategy to reduce interference becomes possible. Interference between the despread pulse field and the totality of the spread pulse fields within the gate-time window can be suppressed by careful choice of codes that yield intensity nulls within the gate-time window. This is equivalent to stating that one chooses an orthogonal code set. Walsh–Hadamard codes can satisfy this requirement; however, all users must be time-synchronized.

D. Fiber Nonlinear Optical Gates: The NOLM

High-speed optical gates that recover rapidly enough to operate at high bit rates are known to the nonlinear optics community. They are based on nonlinear interferometers or four-wave mixing devices. The most common nonlinear materials used in these devices include glass, in the form of single-mode fibers (SMFs), and semiconductor optical amplifiers (SOAs).

An optical interferometer must maintain stability of two optical paths to a small fraction of a wavelength. This demanding stability requirement is accomplished in practice in a fiber-optic Sagnac interferometer, which is called the nonlinear optical loop mirror (NOLM) [50] (Fig. 11). The NOLM has been developed for use as an all-optical ultrafast gate [51]. A single data pulse is incident on port 1 of a 2×2 splitter. The two output ports inject identical copies of the data pulse into each arm of the loop, one circulating in the clockwise (CW) direction and the other in the counterclockwise direction (CCW). In the absence of a clock, the data pulses meet at the splitter with a phase difference such that all the power is directed back out through port 1, hence named "optical loop mirror." If instead, a clock pulse of sufficient intensity is injected into the loop at port 2, in synchrony with the clockwise data pulse, then cross-phase modulation from the gate pulse to the CW pulse accumulates along the loop path to achieve a π phase shift relative to the CCW pulse. Then, the interference between the two at the 2×2 splitter causes the pulse to be output through port 3. The gate width is determined by the clock pulse width and the degree of walk-off between the CW pulse and the clock pulse and can be in the 1–2-ps range. Nonlinear optical gates have been successfully used alone and in combination with nonlinear optical thresholders as well as code selection to obtain spectral efficiencies exceeding 20%, as will be discussed in Section IX.

IX. Multiuser Test-Bed Results

In the last few years, several groups have constructed OCDMA test beds based on spectral encoding and decoding. These test beds incorporate one or more of the encoder/decoder methods mentioned earlier as well as nonlinear optical thresholders and nonlinear optical gates. Several principal research trends can be discerned in the work of several groups during the last decade. One thread of investigation moved toward exploring asynchronous multiuser communication links, or links with relaxed timing requirements such as the use of time slotting to avoid multiuser interference. A second major trend was toward developing demonstration OCDMA links with high spectral efficiency. In order to realize high spectral efficiency, a large number of simultaneous users must be demonstrated and this demands that MUI must be suppressed requiring synchronization of users at the chip level (equal to the despread pulse width) as well as ultrafast gating with the same chip-level precision.

Since spectral OCDMA depends upon precise control of spectral phase of subpicosecond pulses, compensation of link dispersion is critical for maintaining the required spectral-phase codes. Data pulse bandwidths of the order of ~5–10 nm or more are required to support a large number of users each with, for example, a 10-Gb/s data rate assuming a spreading factor of 100. Since a standard SMF has $D = 17$ ps/km/nm, 1 km of uncompensated fiber would broaden a bandwidth-limited pulse by approximately two orders of magnitude, which cannot be despread by the decoding process alone. Both laboratory test-bed experiments and later field trials have shown that dispersion compensation together with dispersion slope compensation has enabled phase-sensitive multiuser spectral OCDMA demonstrations over links many of them tens of kilometers long.

One of the earliest spectral OCDMA test beds was described by Sardesai *et al*. [52] in 1998. This work brought together several subsystems for the first time in spectral OCDMA including fiber-connected and well-characterized liquid crystal SLM-based grating encoders/decoders, dispersion-compensated erbium-doped fiber amplifiers (EDFA), a 2.5-km DSF fiber link with dispersion compensation as shown in Fig. 12. Dispersion slope compensation was also accomplished by adding appropriate third-order spectral-phase-shift compensation in the decoder as evidenced by the shortened cross-correlation signal in Fig. 12(c). The test bed also included a DSF thresholder. The authors measured single-user thresholding with high contrast (~30 db) at the 30-MHz repletion rate of their fiber laser source. Subsequent experiments using this test bed demonstrated error-free operation at 40 Mb/s in the presence of a single asynchronous interference channel [53]. Experiments demonstrating error-free operation of an OCDMA channel in the presence of an overlapping narrow-band WDM channel were also performed [54]. Although these early test-bed results had not yet reported measured error rates at communication data speeds (range, gigabit per second), nonetheless it was a major step forward by showing that spectral-phase encoding of subpicosecond optical pulses at communication wavelengths can be maintained over significant fiber spans and decoded with high fidelity.

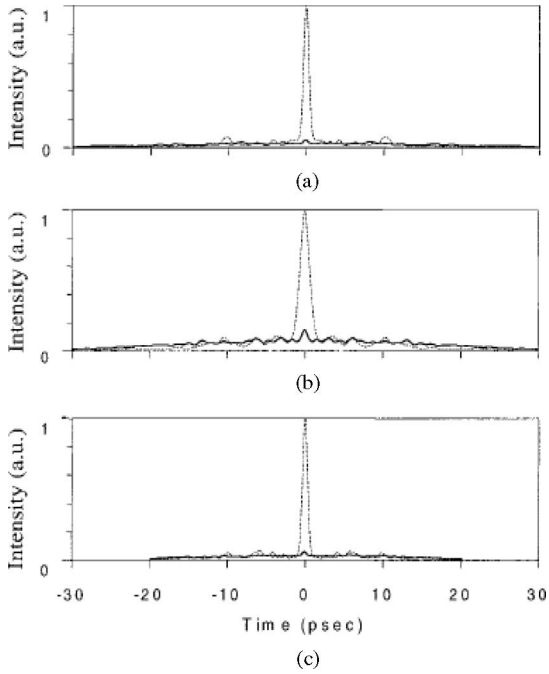

Fig. 12. Intensity autocorrelations for spectral encoding and decoding with a length-63 m-sequence (a) back-to-back, (b) 2.5-km dispersion compensated link, (c) with additional phase trimming using SLM. Dashed line, properly decoded; solid line, improperly decoded. (Sardesi *et al*. [52])

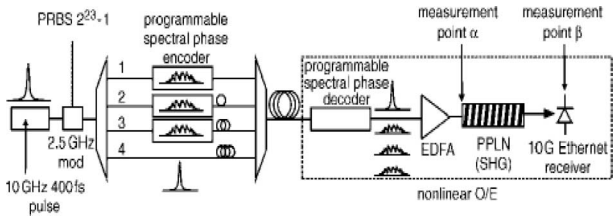

Fig. 13 Four-user OCDMA system test bed. (Jiang *et al*. [55])

A. Simple Access Protocol—Slotted Coordination

Jiang *et al*. [55] expanded the capabilities of the test bed described in [52] by adding the high-sensitivity PPLN waveguide nonlinear optical thresholder and a total of four programmable spectral-phase encoders and were able to demonstrate a four-user OCDMA link. Three encoders were used to create coded data streams, which were added to an unencoded picosecond pulse, which acted as an interferer for the fourth channel. The experimental arrangement is depicted in Fig. 13. A 10-GHz repetition rate fiber laser was modulated at 2.5 GHz with a pseudorandom signal. The authors employed a slotted OCDMA strategy to eliminate time-overlapped contributions to MUI and demonstrated better than 10^{-11} BER at 2.5 Gb/s. Each of the four users' data pulses was assigned one of the four distinct adjacent slots in time sequence. Fig. 14 shows measured cross correlations of the spread pulses, each in their respective time slot, and a decoded data pulse measured at point α in Fig. 13 located before thresholding. Error-free operation was achieved with only ~0.4 pJ/pulse showing that the PPLN thresholder

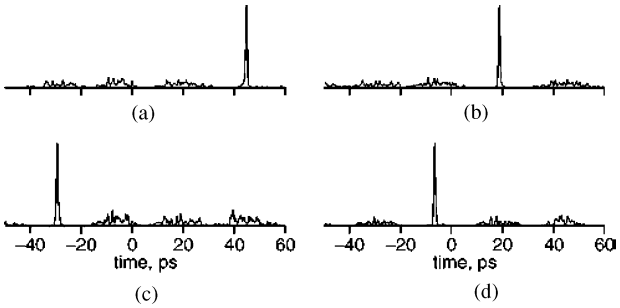

Fig. 14. Intensity cross correlations of properly decoded pulse in each of the four time slots (a)–(d). (Jiang *et al*. [56])

successfully detects the despread pulse while rejecting all of the spread pulses.

In related experiments, Jiang *et al*. showed that phase coding of pulses could be maintained over much longer link results by demonstrating [57] distortionless propagation of 500-fs pulses over a fiber link 50-km long using carefully selected fibers and phase trimming with the spatial light modulator. This work also showed that in this parameter range, polarization-mode dispersion was beginning to affect transmission performance. Error-free operation of two OCDMA channels at 2.5 Gb/s was demonstrated over this 50-km link in a time-slotted coordination scheme [58].

In [56], Jiang *et al*. moved to a four-user demonstration at 10 Gb/s using the same configuration as in Fig. 14. However, careful attention to dispersion compensation, code alignment, etc., allowed a reduction in the pulse energy required to obtain 10^{-11} BER to an impressive 30 fJ! BER data from [56] are shown in Fig. 15. The data in Fig. 15(a) show essentially no power penalty as the number of users is scaled from one to four (the power required at the nonlinear thresholder scales ideally as the number of users). The data in Fig. 15(b) show that all the OCDMA channels perform in a very close to identical way. The achievement of very low-pulse energy requirements is significant in that it demonstrates that scaling a slotted OCDMA system to a large number of users is manageable, at least as far as the power budget is concerned; while the data of Fig. 15 provide an example of OCDMA operation in a regime where very clean interference suppression is achieved.

Assigning unique slots to individual users is an effective strategy to eliminate MUI, and slotting does not require high-precision data-bit-level timing, synchronous detection, or phase-coherent detection. The price paid for this simplicity is that only a limited number of users can be accommodated, especially at high user-data rates and fixed-source pulse widths.

In an expanded discussion, Jiang *et al*. [59] point out that to obtain total system capacities of ~100 Gb/s, code lengths of 127–511 are required as well as shorter pulsewidths (100–300 fs). Shorter pulsewidths permit increased code length, since greater spectral width is available for longer codes. They also note the important tradeoff between capacity and system complexity, especially regarding the degree of necessary timing precision and the degree of coordination required between the transmitter and the receiver. In general, increasing timing coordination and synchronism provides increased user cardinality

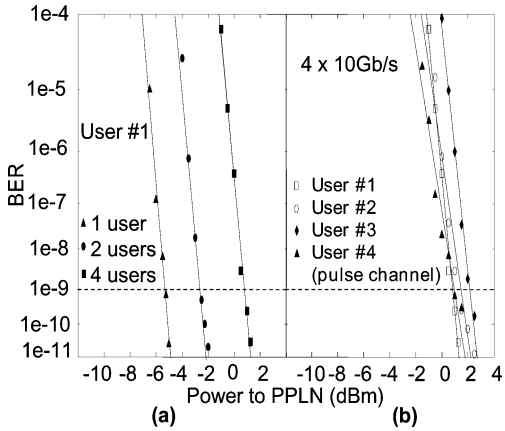

Fig. 15. Performance measurement of 4 × 10 GB/s time-slotted OCDMA system. Powers refer to the values in the PPLN nonlinear discriminator. (a) BER measurements of user 1. The curves shift to higher power in proportion to the number of users, as expected for operation without excess power penalty. (b) BER measurement of all four users. (Jiang *et al*. [56])

and spectral efficiency but at the cost of greater complexity. They projected that high spectral efficiency will likely be possible using full chip-level timing and synchronous gating with chip-level timing required at the receiver.

B. High Spectral Efficiency—Synchronous

Several approaches toward demonstrations of high spectral efficiency have been pursued. All of this work utilizes phase coding and time-synchronous users. Precise temporal gating is also employed in experiments achieving the highest spectral efficiency.

In the first example of such a work, Sotobayashi *et al*. [38], [60] used a programmable transversal filter, which provided three-chip time-domain codes with four-level phase encoding in a TS-OCDMA configuration. By using fast-time gating as well as optical hard thresholding and polarization multiplexing, eight OCDMA users at 40 Gb/s per user were accommodated within a 200-GHz frequency band. Furthermore, because the transversal filter encoder–decoder chips exhibited periodic spectral response at 200-GHz free spectral range, this approach allowed additional transmission channels through a hybrid OCDMA-WDM approach. As a result, this impressive experiment demonstrated 6.4-Tb/s transmission bandwidth (4 OCDMA × 40 WDM × 40 Gb/s) within the 4-THz lightwave C-band. All channels were verified to have BER below 10^{-9}. The 1.6-b/s/Hz spectral efficiency was the highest that had been demonstrated at that time in any form of optical fiber communications.

In the following, we review more recent research involving synchronous spectral-phase encoding. One approach, discussed by Galli *et al*. [25], [26], [61], [62], employs very high-resolution spectral encoders/decoders (VIPA, discussed in Section V) with a free spectral range of 80 GHz and mode or chip spacing as small as 5 GHz in conjunction with synchronous optical gating. Another approach, discussed by Scott *et al*. [46], [49], [67], [69]–[72] used the original grating and lens

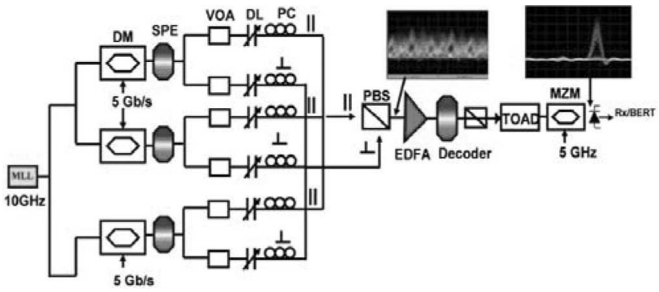

Fig. 16. Experimental arrangement (Agarwal *et al*. [65])

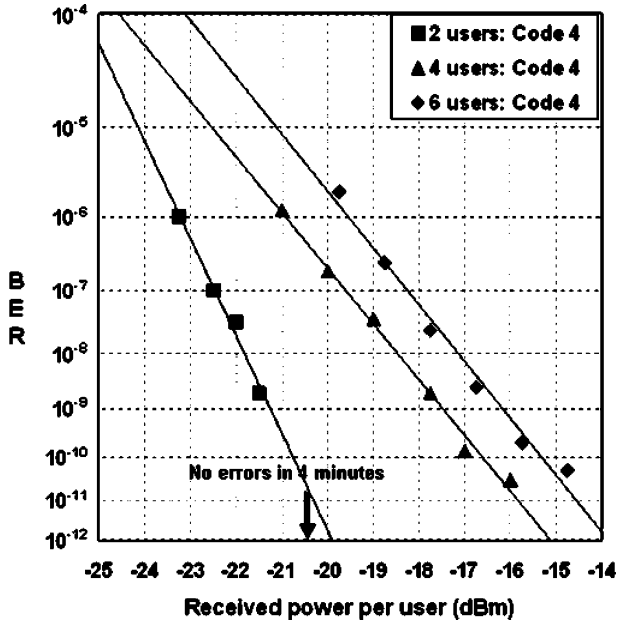

Fig. 17. Measured BER for two-, four-, and six simultaneous users. (Agrawal *et al*. [65])

Fourier transform pulse shapers with spectral bandwidth of 10 nm ($\sim$1.2 THz) and spectral resolution of $\sim$0.1 nm (12.5 GHz). Although all these experiments required synchronism at the transmitter, the earlier experiments [46], [49], [63] done here used optical thresholding, but did not use synchronous gating, while later experiments [67], [69]–[72] employed both gating and thresholding (both implemented via nonlinear fiber optics). Another experiment, described by Jiang *et al*. [64] uses similar laser pulse parameters and bulk optic pulse shapers in conjunction with synchronous transmission and asynchronous thresholding using PPLN waveguides.

1) Narrow-Band Synchronous: The objective of the narrowband, high-resolution approach taken by the authors of [25], [26], [61], and [62] was to demonstrate an OCDMA system that could overlay an all-optical WDM network with narrow-enough bandwidth requirements that OCDMA channels could be switched by transparent optical WDM networks. Their initial implementation [26] of spectral OCDMA used 16 distinct axial modes spaced by 5 GHz, which are filtered from the spectral comb of a mode-locked laser using the VIPA wavelength demultiplexer. Four users were encoded in a configuration that was similar to Fig. 16. Binary-phase Walsh codes were selected from a Hadamard family for the favorable property of zero value of Fourier transforms of the cross correlations for zero delay between pulses. This means that all of the stretched pulses corresponding to the multiple users must be coordinated to arrive at the decoder in time synchronism and the unstretched correctly decoded user pulse must coincide precisely with the null. For the results of [26], synchronism is required comparable to the unstretched data pulse width of $\sim$12.5 ps. The optical gate employed was a terahertz optical asymmetric demultiplexer (TOAD) [66], which is similar conceptually to a NOLM except that an asymmetrically disposed SOA provides optical nonlinearity and the asymmetric location of the SOA enables rapid gating. The gate aperture must also be synchronized with the common null at the middle of each stretched pulse with similar precision, although the authors report timing tolerance of 15 ps with only a modest BER power penalty of 1 dB. With these conditions satisfied, the unstretched pulse of the desired user can ideally be resolved without MUI. The authors were able to obtain better than 10^{-9} BER at 2.5 Gb/s in all cases with a spectral efficiency of 12.5%.

The previously discussed demonstrations of high-resolution spectral OCDMA used the VIPA wavelength demultiplexer, which, similar to gratings, relies on lenses and free-space propagation to reach a focal plane where spectral resolution is optimum. In order to move toward deployable high-spectral-resolution OCDMA network, compact, stable, and easily integrateable demultiplexers need to be developed. One answer to this challenge is the ring-resonator-based integrated decoder discussed in Section VI-B. Recently, Agarwal [65] has demonstrated a six-user coherent OCDMA system employing a fourth-order, eight-frequency bin device each with a passband of 8 GHz. The eight bins were spaced on a 10-GHz frequency grid; thus, the frequency space occupied is only 80 GHz. The output of a 10-GHz mode-locked laser is split by a 1×4 splitter with three of the ouputs modulated by a 5-Gb/s ON–OFF keyed data stream yielding two optical pulses per data bit. Three eight-channel encoders imposed three codes from a Hadamard-8 code set. Polarization multiplexing was used to generate a six-user data stream, which is suitably synchronized, combined with a polarization beam splitter. After decoding with another ring resonator filter, MUI rejection was accomplished with a TOAD gate that extracts the despread desired user. The authors of [65] report that a second Mach–Zehender modulator (Fig. 16) was used to select one of the two optical pulses in the data format, which was found to be important in obtaining the best BER performance as shown in Fig. 17 for user 4. Each coded user was also selected in turn by changing the decoder. Each user code yielded a BER of 5×10^{-11} or better without the aid of FEC. These results imply a spectral efficiency of 0.375 b/s/Hz, the best reported so far in experiments based on spectral encoding. The use of a compact encoder in [65], as in earlier time-domain phase encoding experiments in [60], is an important step toward integrated optical OCDMA transceivers, where the encoder/decoder shrinks from bulk optic tabletop size to a chip size of a few centimeters and points the way toward the potential for a commercially viable, compact OCDMA transceiver.

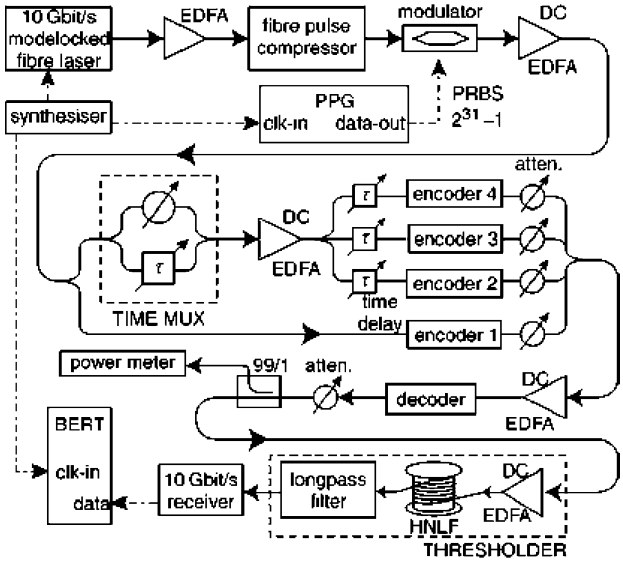

Fig. 18. Two time-slot spectral OCDMA arrangement. The time multiplexer and encoders 2–4 produce six encoded users, three each in two time slots. Encoder 1 generates the desired user and is timed to center in one slot. (Cong *et al*. [63])

2) Broadband Synchronous: In general, the longer the code, the greater the number of users that can be accommodated. In spectral-phase-modulated OCDMA, long codes imply broad spectrum and, thus, short pulses. For example, at 20-Gb/s data rate, with a data format of 1 pulse per bit, the most that a pulse can be spread beneficially is 50 ps, the bit period. The best case would occur if we had a fully orthogonal code set and a receiver that could take full advantage of the orthogonality. If we wanted to accommodate 50 users, then the despread pulse width must be 1 ps or less, which implies the need for a bandwidth of 500 Ghz or greater. Defeating the MUI interference that occurs in any realistic situation requires even greater spreading ratio, i.e., even greater bandwidth.

Recent advances using synchronous spectral OCDMA with larger number of users using optical bandwidths of ~1 THz have recently been demonstrated on an optical test bed. In 2004, Scott *et al*. [46] used free-space optics grating and lens pulse shaper as encoder and decoder, respectively, to demonstrate four-user spectral OCDMA. Their experimental arrangement consisted of a commercial mode-locked fiber laser that produced ~0.5-ps pulses at 10-GHz repetition rate. A special pulse shaper that uses cylindrical optics and a two-dimensional spatial light modulator allowed four user channels to be encoded with each optical path in close proximity, allowing sharing of the same mechanical supports for stability. Walsh–Hadamard codes of length 64 were selected for their individual properties of minimal interference over the entire spread pulse widths. With this choice of codes, a HNLF fiber thresholder was sufficiently robust against MUI to allow error-free operation of a single user in the presence of three interferering users when all four spread pulses were perfectly temporally overlapped and synchronized.

Cong *et al*. [63] extended these results by adding a time multiplexer to add three more channels to adjacent 50-ps-wide slots. Their extended experimental arrangement is shown in Fig. 18.

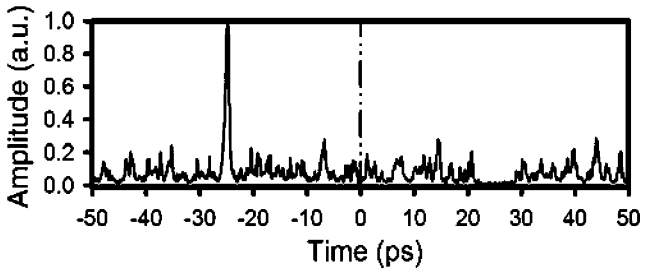

Fig. 19. Cross-correlation measurement of 7-user OCDMA. Slot 1 (negative time), contains temporally despread user and three spread interfering users. Time-slot 2 (positive time) contains three spread interfering users. (Cong *et al*. [63])

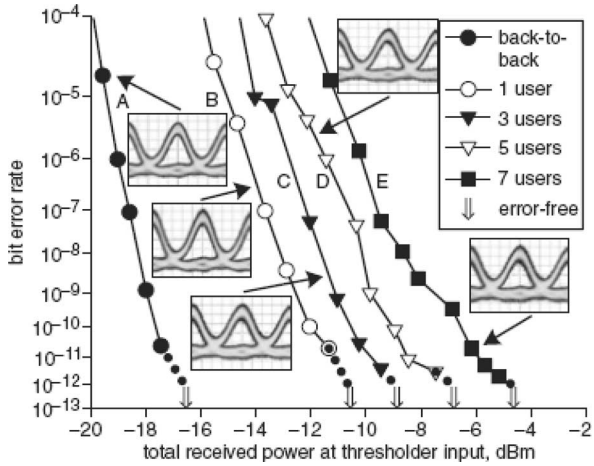

Fig. 20. BER performance as a function of total received power. (Cong *et al*. [63])

A time multiplexer produces two identical copies of the source-modulated pulse train, each separated by 50 ps to form two data slots. The encoder impresses selected Walsh codes on each path and, thus, each time slot contains identical copies of three encoded users. Another encoder imposes yet another different code on a seventh channel, which plays the role of the desired user, that the final encoder will despread. The resulting measured cross correlations are displayed in Fig. 19. The correctly decoded pulse is evident as a spike in the center of time-slot 1. The null in the center of time-slot 2 is a demonstration of the desired properties of the Walsh codes. The fluctuations of the temporal signal owing to optical interference are not evident in this time-averaged measurement. The measured BER versus total power received at the thresholder input for one, three, five, and seven users along with eye diagrams is displayed in Fig. 20. The arrows indicate the total power required to achieve error-free performance. The total capacity of the demonstration link is 70 Gb/s.

Jiang *et al*. [64] described a related experiment but using a modified coding scheme and with PPLN as the thresholder. The test bed was similar to that of Fig. 14, but modified to allow chip-level timing synchronsim in transmission. Owing to the narrow-phase-matching bandwidth in PPLN, the SHG yield strongly depends on the spectral correlation function of the applied field, which can be manipulated based on code.

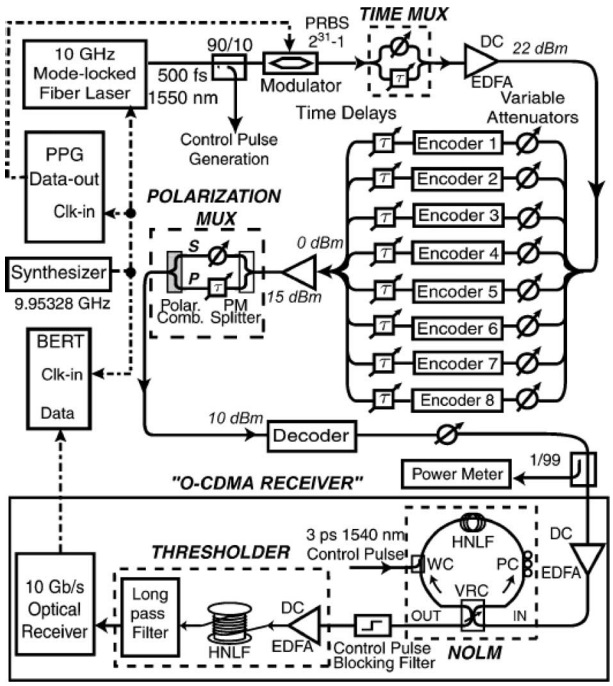

Fig. 21. Sixteen- and 32-user spectral-phase OCDMA network test bed incorporating both time slotting (16- and 32-user) and polarization multiplexing (32-user only). (Cong *et al*. [69])

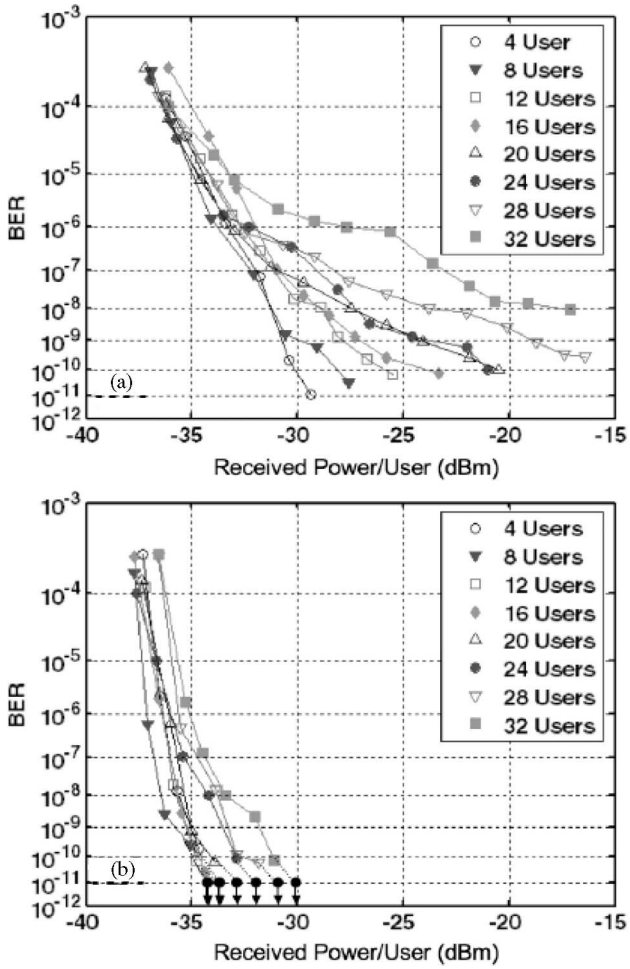

Fig. 22 Comparison of 32-user BER performance (a) without and (b) with FEC. (Hernandez *et al*. [72])

Experiments [47], [68] showed as much as 30-dB suppression of the output signal for a single incorrectly decoded user. By using double-Hadamard codes (two Hadamard codes, one applied to each half of the spectrum), it is possible, in theory, to achieve full orthogonality, which ideally gives zero crosstalk between orthogonal codes and, consequently, full MUI suppression. This property requires chip-level timing coordination as well as spectral intensity equalization. Experiments were performed with three users at 10 Gb/s overlapped in time with chip-level synchronism as well as with four users in a hybrid scheme employing both chip-level synchronism and multiple time slots (e.g., three overlapped users in one slot, one in a different slot, etc.). In all cases, BERs below 10^{-9} were achieved at low pulse energies of $\sim$50 fJ per bit at the PPLN thresholder.

It is important to note that in the previous experiments in this section, strict timing coordination among all users is required to achieve error-free performance. However, no special optical timing constraint was imposed on the thresholder. It was shown in a sequence of experiments [67], [69]–[71] that many more users can be accommodated when a fast optical gate is added just before the thresholder. Fig. 21 shows the culminating experimental arrangement that enabled a 16- and 32-user demonstration with each user's bit rate of 10 Gb/s for an impressive total capacity of 320 Gb/s. A NOLM, gated by a 3-ps control pulse synchronized to the center of one time slot, selects the desired despread user while rejecting MUI from spread users outside the gate time. In these experiments, both NOLM and thresholder were implemented using nonlinear fiber optics. The gating function allowed the addition of five more interfering users in each time slot, which required a total of eight encoders plus one decoder. In this configuration, the test bed supports a total of 16 users and error-free operation was achieved, although at the expense of an MUI-related power penalty of about 7 dB that accumulated as the number of users increased from 10 to 16 users. The addition of a polarization multiplexer doubled the number of users to 32. In this configuration, a BER of 10^{-10} was achieved for 24 users and 10^{-8} for 32 users.

Hernandez *et al*. [72] extended the 32-channel performance by adding FEC to the test bed. The FEC encoder was inserted in ON-OFF-keyed electronic data stream just ahead of the $LiNbO_3$ Mach–Zehnder modulator. The FEC decoder was added just after the optical receiver. The data stream may then be optionally FEC-encoded using a well-known Reed–Solomon code [RS(255,239)]. When FEC is in use, the data rate is lowered to 9.250698 Gb/s to accommodate the 6% coding overhead, maintaining OC-192 into the modulator. Fig. 22 presents a comparison between the 32-user BER performance plotted against received power per user, without and with FEC.

The FEC was successful in reducing the BER to less than 10^{-11} for all 32 users. The non-FEC system with full spectrum has a throughput of 278.7 Gb/s (28 users at BER $< 10^{-9}$) using 19 nm of bandwidth, and, thus, has 0.12-b/s/Hz spectral

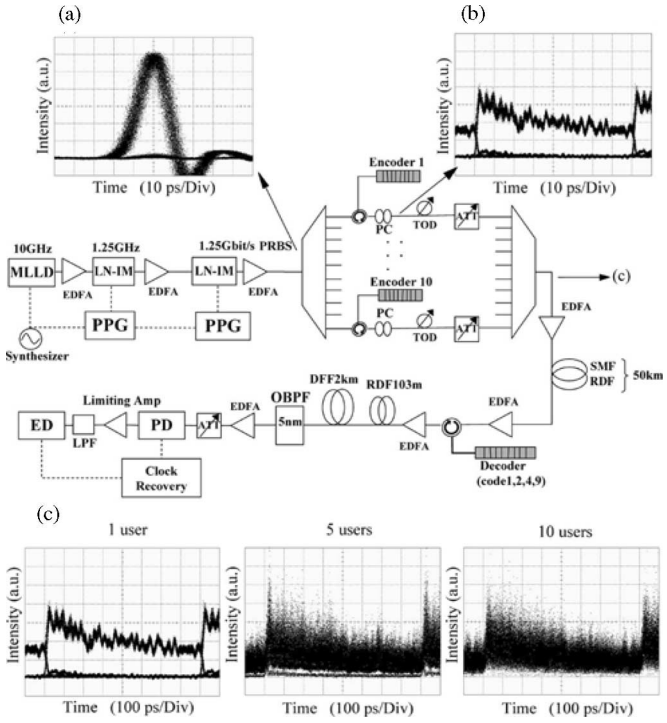

Fig. 23. Ten-user asynchronous TS-OCDMA transmission experiment at 1.25 Gb/s/user with 511-chip SSFBG encoders/decoders. (a) Eye diagram after intensity modulation. (b) Eye diagram after encoding. (c) Eye diagram for different numbers of combined users. PPG, pseudorandom pattern generator; PC, polarization controller; TOD: tunable optical delay; PD, photodiode; LPF, low-pass filter. (Hamanaka *et al*. [39])

efficiency. In order to improve the spectral efficiency, the spectrum was narrowed to 12 nm, which is easily accomplished with an aperture in the decoder. The FEC maintained error-free performance with all 32 users. The narrower band implementation successfully maintains the 296-Gb/s throughput resulting in a spectral efficiency of 0.20-b/s/Hz, or a 58% increase over the wideband system.

C. Simple Access Protocol—Asynchronous TS-OCDMA

Using SSFBG encoders/decoders, as described in Section VII-B, Hamanaka *et al.* published results from an impressive ten-user, truly asynchronous transmission experiment [39]. Fig. 23 shows the experimental setup. A mode-locked laser diode (MLLD) produces 1.8-ps pulses at a 10-GHz repetition rate and centered at 1550 nm. This pulse train is intensity modulated by a $LNbO_3$ modulator (LN-IM) with a $2^{31}-1$ pseudorandom bit sequence (PRBS) at 1.25 Gb/s. The eye diagram of this signal is shown in Fig. 23(a). After amplification by an EDFA, the signal is equally split into ten signals and encoded by ten separate SSFBG encoders connected via optical circulators. The encoders impress a 511-chip phase code based on Gold codes. Fig. 23(b) shows the signal encoded by Encoder 1. The signals were then combined, amplified, and propagated through 50 km of SMF. Fig. 23(c) shows the eye diagram just after they are combined for the single-user-, five-user-, and ten-user cases. A reverse dispersion fiber (RDF) is used to compensate for dispersion

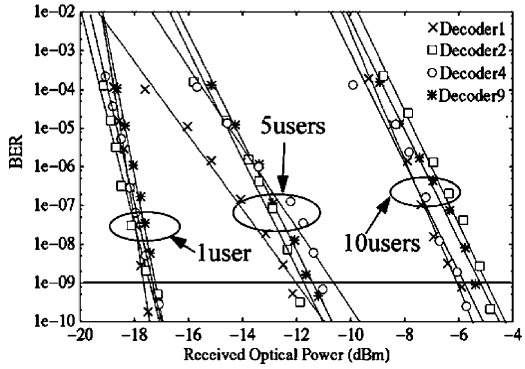

Fig. 24. Measured BER at 1.25 Gb/s/user for TS-OCDMA 50-km transmission using 511-chip SSFBG encoder/decoder. (Hamanaka *et al*. [39])

of the SMF before the combined signals are decoded by an SSFBG decoder. The decoder output passes through a nonlinear optical thresholder based on dispersion-flattened fiber (DFF). The high peak power of the correctly decoded signal generates additional spectra through supercontinuum generation in the DFF similar to schemes described in Section VII-A [45], [46]. A 5-nm optical bandpass filter (OBPF) is used to select a portion of the newly generated spectrum, which is then passed on to the clock and data recovery receiver. The measured BER statistics are shown in Fig. 24 for one user, five users, and ten users after 50-km transmission. Four different encoders are decoded (Encoders 1, 2, 4, and 9) to show the variation in BER for different codes. In the worst case scenario for the TS-OCDMA network, error-free transmission was achieved for up to ten users for the four different decoders. The success of the Hanamaka asynchronous experiment may be attributed to the ability of the SSFBG to use very long code words (511 chip) and, thus, produce large spreading ratios.

In a rather recent dramatic advance, Wang *et al*. [73] have demonstrated 12-user asynchronous time-spreading OCDMA at 10.71 Gb/s using an AWG-based multiport encoder–decoder. Unlike the case of pure spectral-phase encoding where all decoded pulses have the same energy, an AWG time/phase encoder–decoder combination was configured so that the correctly decoded pulse has more energy than any of the decoded signals. This energy reduction reduces MUI allowing shorter code lengths and, thus, higher bit rates without requiring femtosecond pulses. The authors of [73] report raw BER of $\sim 10^{-4}$, which was improved to 10^{-14} by Reed–Solomon FEC. Note, however, that because the different output codes have little spectral overlap with each other (when viewed with sufficiently high spectral resolution), this approach is quite different than other OCDMA schemes considered here (where all codes have complete or at least very strong spectral overlap).

D. Security

The possibility of enhanced information confidentiality is frequently mentioned as a potential feature of OCDMA. One might argue that in OCDMA, information bits are spread into unrecognizable noise-like temporal signatures and the codes that generate this "noise" can, in principle, be made very long and

presumably time consuming to break. However, an OCDMA network uses codes as addresses and often employs simple ON–OFF keying (OOK) for data modulation. In this case, in which no special attention is paid to ensuring security, the network in itself is not at all secure. In the case of OOK, an eavesdropper need only listen [59], [74], [75] with an adequately fast receiver in a position in the network where a single data stream is present, such as upstream traffic in a star network. Even if all such single-user locations are physically secured by other means, it is not hard for an eavesdropper to guess that codes are being used as addresses and, then, a search only needs scan through the small number of known orthogonal and pseudoorthogonal code sets, many of which are well known.

In an assessment of security and confidentiality issues in OCDMA, Shake [74], [75] proposed code switching as a means to make the data stream unreadable by a fast receiver. In this scheme, a "mark" is represented by one distinct code and a "space" by another code. In this manner, the energy in each symbol will nominally be the same. Thus, a phase-coded data stream will look to the energy detector of the eavesdropper as a sequence of "marks" with the actual data "hidden" in the change in spectral phase. Leaird *et al.* [76] demonstrated code-switching in a simple slot-level timing link using two encoders, each with a distinct code. When the authorized OCDMA decoder is tuned to the conjugate code of the "mark," then it is detected as a destretched pulse while the "space" is rejected as a noise-like waveform. Significantly, a clear "eye" diagram showed that the data bit stream was then recovered. While this strategy was successful in hiding the data stream, the authors of [76] point out that there are other vulnerabilities in the signaling and encoding schemes. In particular, Jiang *et al.* [77] demonstrated experimentally two more vulnerabilities. One results from a fundamental property of spectral encoding that causes intensity dips in the spectrum at each frequency where a code phase transition occurs. Since the "Mark" code differs from the "space" code, many of the dips occur at different spectral locations. Therefore, a simple narrow-band filter can be tuned across the spectrum until an eye opens when a dip is encountered in one code, which is not present in the other. This vulnerability can be minimized by adding another cascaded spectral-phase modulator that places additional phase transitions at the vulnerable spectral locations. The second vulnerability considered by [77] arises when a differential phase-shift keying (DPSK) detector is employed. A DPSK detector interferometrically compares adjacent pulses. When adjacent bits are identical, they can interfere constructively to give a large signal. When they differ, the interference is small because the output is averaged over different spectral chips. In this manner, the supposedly hidden transmitted sequence of "marks" and "spaces" may be discerned. These two physical layer vulnerabilities are likely not the only ones that need to be defeated. Achieving *bone fide* security at the physical layer of OCDMA remains an unsolved problem.

One interesting approach that has recently been proposed [78] involves overlaying a covert channel onto a host channel, both of which may be OCDMA-encoded. The key new point is that the covert channel has power spectral density below the noise floor [e.g., amplified spontaneous emission ASE)] in the fiber system, making it difficult to detect directly. It is proposed that with sufficiently long codes, the processing gain of an OCDMA decoder should pull the signal above the noise floor, allowing satisfactory detection.

E. Passive Code Translation

To establish arbitrary connection among a large number of users in a single network requires a corresponding large number of user addresses. In spectral OCDMA, physical device constraints limit the potential number of addresses. However, if the network is physically divided into separate smaller clusters of users that are connected by a "bridge" with code-translation capability, then addresses in other segments can be accessed. Such an architecture was discussed by Kitayama in [79]; however, it employed optoelectronic conversion. A strength of spectral OCDMA is the relative ease with which a phase code may be converted to another code by a simple passive optical process; namely, through the use of an encoder as a bridging element. Jiang *et al.* [80] experimentally demonstrated code translation through multiple stages and investigated degradation arising from spectral dips. Mendenez *et al.* [81] investigated applications of cascaded phase-code translation to network architectures, including interconnected star networks with passive routing using code translation, ring architectures, and code-scrambling applications. Passive, all-optical code translation is likely to play an important role driving spectral OCDMA toward practical application.

F. Field Trials

Until recently, most OCDMA demonstrations were confined to the controlled environment of university or industry research laboratory test beds and bulky free space optical encoders and decoders were used along with fiber-based components. Furthermore, when long fiber stretches were employed in the test-bed demonstrations, the experimenters had access to modern fibers and were able to optimize the dispersion of the fiber run in question. Recently, Hernandez *et al.* [82] demonstrated a two-user OCDMA link over 80.8 km of BOSSNET in the Boston area. They employed fully integrated polarization-independent, silica AWG devices as spectral-phase encoders that support code lengths of up to 64. This experiment also used an optical frequency comb generator cascaded with a dispersion decreasing fiber to produce over 120 optical comb lines spaced at 20 GHz. Data was modulated at 2.5 GHz and sent to two multiport AWGs separated by phase modulators. Two user codes were generated by splitting the modulated input to two different input ports of the AWG encoder producing two bit-shifted 63-chip m-sequence encoded data streams. The encoded data streams were combined and sent to the in-ground field fiber loop-back of total length 80.8 km. The link consisted largely of LEAF fiber and dispersion compensation fiber (DCF). Measurement of the loop dispersion revealed, after compensating for residual dispersion with a short stretch of the DCF fiber, a dispersion slope of 6 ps/nm^2, which, if uncompensated, would have broadened the despread pulse to the point that the thresholder could not distinguish it from an interfering pulse. Furthermore, phase

correction in the encoder/decoder [57] was not possible for this large value of dispersion slope.

The link dispersion slope was successfully compensated with a bulk optics pulse shaper with a flexible mirror in the Fourier plane [83]. The mirror was a thin ribbon cut from an optically ground and polished aluminum sheet. The mirror was supported by pressure from four rigid steel shafts, two on each side of the ribbon, disposed in such a way that the force flexes the ribbon into a cubic bend. It is interesting to note, that unlike a pixelated cubic phase shift provided by an SLM, which was used in the 50-km laboratory dispersion compensation experiments of [55], the bent mirror deflects frequency components laterally on the Fourier lens. As a result, this device offers continuous phase variation. This device was able to provide up to 5.5-ps/nm^2 dispersion-slope compensation and two-user BERs better than 10^{-9} were obtained using only the HNLF nonlinear fiber thresholder in a time-slotted scheme without synchronous gating. The same group successfully demonstrated a 150-km field trial of security-enhanced spectral OCDMA links using bright-code/dark-code data modulation at 2.5-Gb/s/user incorporating integrated silica AWG encoders [84]. Again, dispersion slope compensation was accomplished with the bent-mirror pulse shaper. The link consisted of 150 km of field fiber (circa 1990) that spans between Burlingame, CA, in Sprint Nextel Advanced Technology Laboratory, and a point-of-presence in Palo Alto, CA. At these large distances, polarization dispersion emerged as significant physical layer impairment. Nonetheless, two simultaneous users requiring a total of four encoders with FEC achieved a BER of 10^{-11}.

X. Conclusion

Coherent OCDMA research using laboratory test beds based on fiber-pigtailed freespace optic spectral-phase encoders and decoders have successfully explored a range of architectures from highly coordinated synchronous point-to-point systems to those with minimal or slot-level synchronism. The results show that coherent interference between users is a very important impairment that must be carefully minimized through the use of synchronous optical gates, time slotting, or careful code selection. The experiments with time-spreading OCDMA using SSFBGs have convincingly verified experimentally that the use of very long codes improves asynchronous performance dramatically by reducing coherent interference. In addition, several field trials have shown that even when using fiber-in-the-ground, good performance can be obtained. Unless high-resolution freespace encoders can be shrunk to the size of a small disk drive, and built at low cost, we look toward the development of planar waveguide-based integrated encoders, such as those recently demonstrated, that are based on InP or silica AWGs and microring resonators. The challenge is to build low-loss devices with high resolution that can support long codes and ultimately be able to reconfigure codes rapidly. We have seen the development of high-sensitivity threshold detectors based on PPLN, an important development considering the basic star topology used for a multiuser LAN based on OCDMA. Just as in wireless CDMA, FEC will likely play a large role in OCDMA, especially in asynchronous systems. OCDMA would benefit significantly from the rapid development of low-cost, high-speed silicon electronics for future 10 Gb and faster FEC circuits.

Acknowledgment

One of the authors (J.P.H.) thanks Z. Ding, S. J. Ben Yoo, and B. H. Kolner for many stimulating discussions. He also acknowledges the expert experimental skills of R. Scott, W. Cong, V. J. Hernandez, N. Fontaine, C. Yang, and K. Li. Another author (A.M.W.) thanks D. E. Leaird, Z. Jiang, D.-S. Seo, and S.-D. Yang for collaboration on OCDMA experiments and M. M. Fejer, C. Langrock, and R. V. Roussev for collaboration on PPLN nonlinear processing devices.

References

[1] A. Viterbi, "Spread spectrum communications—myths and realities," *IEEE Commun. Mag.*, vol. 17, no. 3, pp. 11–18, May 1979.

[2] R. Pickholtz, D. Schilling, and L. Milstein, "Theory of spread-spectrum communications–a tutorial," *IEEE Trans. Commun.*, vol. COM-30, no. 5, pp. 855–884, May 1982.

[3] A. Viterbi, "When not to spread spectrum—a sequel," *IEEE Commun. Mag.*, vol. 23, no. 4, pp. 12–17, Apr. 1985.

[4] L. B. Milstein, "Interference rejection techniques in spread spectrum communications," *Proc. IEEE*, vol. 76, no. 6, pp. 657–671, Jun. 1988.

[5] K. S. Gilhousen, I. M. Jacobs, R. Padovani, A. J. Viterbi, L. A. Weaver, Jr., C. E. Wheatley, III, Q. Inc, and C. A. San Diego, "On the capacity of a cellular CDMA system," *IEEE Trans. Veh. Technol.*, vol. 40, no. 2, pp. 303–312, May 1991.

[6] R. Dixon, "Why spread spectrum?," *Commun. Soc.: Dig. News Events Interest Commun. Eng.*, vol. 13, no. 4, pp. 21–25, Jul. 1975.

[7] Q. Bi, "Performance analysis of a CDMA cellular system," in *Proc. IEEE 42nd Veh. Technol. Conf.*, 1992, pp. 43–46.

[8] T. R. Giallorenzi and S. G. Wilson, "Multiuser ML sequence estimator for convolutionally coded asynchronous DS-CDMA systems," *IEEE Trans. Commun.*, vol. 44, no. 8, pp. 997–1008, Aug. 1996.

[9] P. D. Alexander, M. C. Reed, J. A. Asenstorfer, and C. B. Schlegel, "Iterative multiuser interference reduction: Turbo CDMA," *IEEE Trans. Commun.*, vol. 47, no. 7, pp. 1008–1014, Jul 1999.

[10] A. J. Viterbi, "Wireless digital communication: A view based on three lessons learned," *IEEE Commun. Mag.*, vol. 29, no. 9, pp. 33–36, Sept. 1991.

[11] J. Y. Hui, "Pattern code modulation and optical decoding—a novel code-division multiplexing technique for multifiber networks," *IEEE J. Sel. Areas Commun.*, vol. SAC-3, no. 6, pp. 916–927, Nov. 1985.

[12] S. Tamura, S. Nakano, and K. Okazaki, "Optical code-multiplex transmission by Gold sequences," *J. Lightw. Technol.*, vol. LT-3, no. 1, pp. 121–127, Feb. 1985.

[13] P. R. Prucnal, M. A. Santoro, and T. R. Fan, "Spread spectrum fiber-optic local area network using optical processing," *J. Lightw. Technol.*, vol. LT-4, no. 5, pp. 547–554, May 1986.

[14] J. A. Salehi, "Code division multiple-access techniques in optical fiber networks—Part I: Fundamental principles," *IEEE Trans. Commun.*, vol. 37, no. 8, pp. 824–833, Aug. 1989.

[15] J. A. Salehi and C. A. Brackett, "Code division multiple-access techniques in optical fiber networks—Part II: Systems performance analysis," *IEEE Trans. Commun.*, vol. 37, no. 8, pp. 834–842, Aug. 1989.

[16] J. P. Heritage, A. M. Weiner, and R. N. Thurston, "Picosecond pulse shaping by spectral phase and amplitude manipulation," *Opt. Lett.*, vol. 10, pp. 609–611, 1985.

[17] A. M. Weiner, J. P. Heritage, and R. N. Thurston, "Synthesis of phase coherent, picosecond optical square pulses," *Opt. Lett.*, vol. 11, pp. 153–155, 1986.

[18] R. N. Thurston, J. P. Heritage, A. M. Weiner, and W. J. Tomlinson, "Analysis of picosecond pulse shape synthesis by spectral masking in a grating pulse compressor," *IEEE J. Quantum Electron.*, vol. QE-22, no. 5, pp. 682–696, May 1986.

[19] A. M. Weiner, J. P. Heritage, and E. M. Kirschner, "High-resolution femtosecond pulse shaping," *J. Opt. Soc. Am. B, Opt. Phys.*, vol. 5, pp. 1563–1572, Aug. 1988.

[20] A. M. Weiner, J. P. Heritage, and J. A. Salehi, "Encoding and decoding of femtosecond pulses," *Opt. Lett.*, vol. 13, pp. 300–302, 1988.

[21] J. A. Salehi, A. M. Weiner, and J. P. Heritage, "Coherent ultrashort light pulse code-division multiple access communication systems," *J. Lightw. Technol.*, vol. 8, no. 3, pp. 478–491, Mar. 1990.

[22] X. Wang and K. Kitayama, "Analysis of beat noise in coherent and incoherent time-spreading OCDMA," *J. Lightw. Technol.*, vol. 22, no. 10, pp. 2226–2235, Oct. 2004.

[23] D. J. Hajela and J. A. Salehi, "Limits to the encoding and bounds on the performance of coherent ultrashort light pulse code-division multple-access systems," *IEEE Trans. Commun.*, vol. 40, no. 2, pp. 325–336, Feb. 1992.

[24] A. M. Weiner, "Femtosecond pulse shaping using spatial light modulators," *Rev. Sci. Instrum.*, vol. 71, pp. 1929–1960, 2000.

[25] S. Etemad, T. Banwell, S. Galli, J. Jackel, R. Menendez, P. Toliver, J. Young, P. Delfyett, C. Price, and T. Turpin, "Optical-CDMA incorporating phase coding of coherent frequency bins: Concept, simulation, experiment," presented at the Opt. Fiber Commun. Conf., Los Angeles, CA, 2004.

[26] S. Etemad, P. Toliver, R. Menendez, J. Young, T. Banwell, S. Galli, J. Jackel, P. Delfyett, C. Price, and T. Turpin, "Spectrally efficient optical CDMA using coherent phase-frequency coding," *IEEE Photon. Technol. Lett.*, vol. 17, no. 4, pp. 929–931, Apr. 2005.

[27] M. Shirasaki, "Large angular dispersion by a virtually imaged phased array and its application to a wavelength demultiplexer," *Opt. Lett.*, vol. 21, pp. 366–368, 1996.

[28] S. Xiao, A. M. Weiner, and C. Lin, "A dispersion law for virtually imaged phased-array spectral dispersers based on paraxial wave theory," *IEEE J. Quantum Electron.*, vol. 40, no. 4, pp. 420–426, Apr. 2004.

[29] S. Xiao, A. M. Weiner, and C. Lin, "Experimental and theoretical study of hyperfine WDM demultiplexer performance using the virtually imaged phased-array (VIPA)," *J. Lightw. Technol.*, vol. 23, no. 3, pp. 1456–1467, Mar. 2005.

[30] G. H. Lee, S. Xiao, and A. M. Weiner, "Optical dispersion compensator with $>$4000-ps/nm tuning range using a virtually imaged phased array (VIPA) and spatial light modulator (SLM)," in *IEEE Photon. Technol. Lett.*, vol. 18, no. 17, pp. 1819–1821, Sep. 2006.

[31] H. Tsuda, H. Takenouchi, T. Ishii, K. Okamoto, T. Goh, K. Sato, A. Hirano, T. Kurokawa, and C. Amano, "Spectral encoding and decoding of 10 Gbit/s femtosecond pulses using high resolution arrayed-waveguide grating," *Electron. Lett.*, vol. 35, pp. 1186–1188, 1999.

[32] R. G. Broeke, J. Cao, N. K. Fontaine, C. Ji, N. Chubun, F. Olsson, S. Lourdudoss, B. H. Kolner, J. P. Heritage, and S. J. B. Yoo, "Phase characterization of an InP based optical-CDMA encoder using frequency-resolved optical gating (FROG)," in *Proc. 18th Annu. Meeting IEEE Lasers Electro-Opt. Soc.*, 2005, pp. 140–141.

[33] J. Cao, R. G. Broeke, N. K. Fontaine, C. Ji, Y. Du, N. Chubun, K. Aihara, A. V. Pham, F. Olsson, S. Lourdudoss, and S. J. B. Yoo, "Demonstration of spectral phase O-CDMA encoding and decoding in monolithically integrated arrayed-waveguide-grating-based encoder," *IEEE Photon. Technol. Lett.*, vol. 18, no. 24, pp. 2602–2604, Dec. 2006.

[34] J. Chen, R. G. Broeke, Y. Du, C. Jing, N. Chubun, P. Bjeletich, F. Olsson, S. Lourdudoss, R. Welty, C. Reinhardt, P. L. Stephan, and S. J. B. Yoo, "Monolithically integrated InP-based photonic chip development for O-CDMA systems," *IEEE J. Sel. Topics Quantum Electron.*, vol. 11, no. 1, pp. 66–77, Jan.–Feb. 2005.

[35] C. Ji, N. Chubun, R. G. Broeke, J. Cao, Y. Du, P. Bjeletich, and S. J. B. Yoo, "Electrical subharmonic hybrid mode locking of a colliding pulse mode-locked laser at 28 GHz," *IEEE Photon. Technol. Lett.*, vol. 17, no. 7, pp. 1381–1383, Jul. 2005.

[36] Y. Du, T. Tekin, R. G. Broeke, N. Chubun, C. Ji, J. Cao, S. J. B. Yoo, K. Y. Liou, J. R. Lothian, S. Vatanapradit, S. N. G. Chu, B. Patel, W. S. Hobson, D. V. Tishinin, and W. T. Tsang, "A novel monolithically integrated Mach–Zehnder wavelength converter using cross modulation in electro-absorber," in *Proc. 31st Eur. Conf. Opt. Commun.*, 2005, pp. 361–362.

[37] A. Agarwal, P. Toliver, R. Menendez, S. Etemad, J. Jackel, J. Young, T. Banwell, B. E. Little, S. T. Chu, C. Wei, C. Wenlu, J. Hryniewicz, F. Johnson, D. Gill, O. King, R. Davidson, K. Donovan, and P. J. Delfyett, "Fully programmable ring-resonator-based integrated photonic circuit for phase coherent applications," *J. Lightw. Technol.*, vol. 24, no. 1, pp. 77–87, Jan. 2006.

[38] H. Sotobayashi, W. Chujo, and K. Kitayama, "Highly spectral-efficient optical code-division multiplexing transmission system," *IEEE J. Sel. Topics Quantum Electron.*, vol. 10, no. 2, pp. 250–258, Mar.–Apr. 2004.

[39] T. Hamanaka, X. Wang, N. Wada, A. Nishiki, and K. Kitayama, "Ten-user truly asynchronous gigabit OCDMA transmission experiment with a 511-chip SSFBG en/decoder," *J. Lightw. Technol.*, vol. 24, no. 1, pp. 95–102, Jan. 2006.

[40] X. Wang, K. Matsushima, A. Nishiki, N. Wada, and K.-I. Kitayama, "High reflectivity superstructured FBG for coherent optical code generation and recognition," *Opt. Express*, vol. 12, pp. 5457–5468, 2004.

[41] B. J. Eggleton, P. A. Krug, L. Poladian, and F. Ouellette, "Long periodic superstructure Bragg gratings in optical fibres," *Electron. Lett.*, vol. 30, pp. 1620–1622, 1994.

[42] T. Erdogan, "Fiber grating spectra," *J. Lightw. Technol.*, vol. 15, no. 8, pp. 1277–1294, Aug. 1997.

[43] P. C. Teh, P. Petropoulos, M. Ibsen, and D. J. Richardson, "A comparative study of the performance of seven- and 63-chip optical code-division multiple-access encoders and decoders based on superstructured fiber Bragg gratings," *J. Lightw. Technol.*, vol. 19, no. 9, pp. 1352–1365, Sep. 2001.

[44] X. Wang, K. Matsushima, K. Kitayama, A. Nishiki, N. Wada, and F. Kubota, "High-performance optical code generation and recognition by use of a 511-chip, 640-Gchip/s phase-shifted superstructured fiber Bragg grating," *Opt. Lett.*, vol. 30, pp. 355–357, Feb. 2005.

[45] H. P. Sardesai and A. M. Weiner, "Nonlinear fibre-optic receiver for ultrashort pulse code division multiple access communications," *Electron. Lett.*, vol. 33, pp. 610–611, Mar. 1997.

[46] R. P. Scott, W. Cong, K. Li, V. J. Hernandez, J. P. Heritage, B. H. Kolner, and S. J. B. Yoo, "Demonstration of an error-free 4 $\times$ 10 Gb/s multiuser SPECTS O-CDMA network testbed," *IEEE Photon. Technol. Lett.*, vol. 16, no. 9, pp. 2186–2188, Sep. 2004.

[47] Z. Zheng, A. M. Weiner, K. R. Parameswaran, M. H. Chou, and M. M. Fejer, "Low-power spectral phase correlator using periodically poled $LiNbO_3$ waveguides," *IEEE Photon. Technol. Lett.*, vol. 13, no. 4, pp. 376–378, Apr. 2001.

[48] M. H. Chou, I. Brener, M. M. Fejer, E. E. Chaban, and S. B. Christman, "1.5- μm m-band wavelength conversion based on cascaded second-order nonlinearity in $LiNbO_3$ waveguides," in *IEEE Photon. Technol. Lett.*, vol. 11, no. 6, pp. 653–655, Jun. 1999.

[49] V. J. Hernandez, Y. Du, W. Cong, R. P. Scott, K. Li, J. P. Heritage, Z. Ding, B. H. Kolner, and S. J. B. Yoo, "Spectral phase encoded time spreading (SPECTS) optical code division multiple access for terabit optical access networks," *J. Lightw. Technol.*, vol. 22, no. 11, pp. 2671–2679, Nov. 2004.

[50] N. J. Doran and D. Wood, "Nonlinear-optical loop mirror," *Opt. Lett.*, vol. 13, pp. 56–58, 1988.

[51] K. J. Blow, N. J. Doran, and B. P. Nelson, "Demonstration of the nonlinear Fiber loop mirror as an ultrafast all-optical demultiplexer," *Electron. Lett.*, vol. 26, pp. 962–964, 1990.

[52] H. P. Sardesai, C. C. Chang, and A. M. Weiner, "A femtosecond code-division multiple-access communication system test bed," *J. Lightw. Technol.*, vol. 16, no. 11, pp. 1953–1964, Nov. 1998.

[53] S. Shen, A. M. Weiner, G. Sucha, and M. L. Stock, "Bit-error-rate performance of ultrashort-pulse optical CDKA detection under multi-access interference," *Electron. Lett.*, vol. 36, pp. 1795–1797, 2000.

[54] S. Shen and A. M. Weiner, "Suppression of WDM interference for error-free detection of ultrashort-pulse CDMA in spectrally overlaid hybrid WDM-CDMA operation," *IEEE Photon. Technol. Lett.*, vol. 13, no. 1, pp. 82–84, Jan. 2001.

[55] Z. Jiang, D. Seo, S.-D. Yang, D. E. Leaird, A. M. Weiner, R. V. Roussev, C. Langrock, and M. M. Fejer, "Spectrally coded O-CDMA system with four users at 2.5 Gbit/s using low power nonlinear processing," *Electron. Lett.*, vol. 40, pp. 623–625, May 2004.

[56] Z. Jiang, D. Seo, S. Yang, D. E. Leaird, R. V. Roussev, C. Langrock, M. M. Fejer, and A. M. Weiner, "Four-user 10-Gb/s spectrally phase-coded O-CDMA system operating at $\sim$30 fJ/bit," *IEEE Photon. Technol. Lett.*, vol. 17, no. 3, pp. 705–707, Mar. 2005.

[57] Z. Jiang, S. D. Yang, D. E. Leaird, and A. M. Weiner, "Fully dispersion-compensated $\sim$500 fs pulse transmission over 50 km single-mode fiber," *Opt. Lett.*, vol. 30, pp. 1449–1451, Jun. 2005.

[58] S.-D. Jiang, D. Yang, D. E. Leaird, A. M. Weiner, C. Roussev, C. Langrock, and M. M. Fejer, "Fullly dispersion compensated $\sim$500 fs pulse transmission over 50 km SMF and application to ultrafast O-CDMA," presented at the Conf. Lasers Electro-Opt., 2005, Paper CFK2.

[59] Z. Jiang, D. S. Seo, S. D. Yang, D. E. Leaird, R. V. Roussev, C. Langrock, M. M. Fejer, and A. M. Weiner, "Four-user, 2.5-Gb/s, spectrally coded OCDMA system demonstration using low-power nonlinear processing," *J. Lightw. Technol.*, vol. 23, no. 1, pp. 143–158, Jan. 2005.

[60] H. Sotobayashi, W. Chujo, and K. Kitayama, "1.6-b/s/Hz 6.4-Tb/s QPSK-OCDM/WDM (4 OCDM × 40 WDM × 40 Gb/s) transmission experiment using optical hard thresholding," *IEEE Photon. Technol. Lett.*, vol. 14, no. 4, pp. 555–557, Apr. 2002.
[61] S. Galli, R. Menendez, P. Toliver, T. Banwell, J. Jackel, J. Young, and S. Etemad, "DWDM-compatible spectrally phase encoded optical CDMA," presented at the IEEE Global Telecommun. Conf., Dallas, TX, 2004.
[62] P. Toliver, J. Young, J. Jackel, T. Banwell, R. Menendez, S. Galli, and S. Etemad, "Optical network compatibility demonstration of O-CDMA based on hyperfine spectral phase coding," presented at the 2004 IEEE LEOS Annu. Meeting Conf. Proc., Rio Grande, Puerto Rico, Nov. 7–11.
[63] W. Cong, R. P. Scott, V. J. Hernandez, K. Li, J. P. Heritage, B. H. Kolner, and S. J. B. Yoo, "High performance 70 Gb/s SPECTS optical-CDMA network testbed," *IEE Electron. Lett.*, vol. 40, pp. 1439–1440, Oct. 2004.
[64] Z. Jiang, D. S. Seo, D. E. Leaird, A. M. Weiner, R. V. Roussev, C. Langrock, and M. M. Fejer, "Multi-user, 10 Gb/s spectrally phase coded O-CDMA system with hybrid chip and slot-level timing coordination," *IEICE Electron. Express*, vol. 1, pp. 398–403, Oct. 2004.
[65] A. Agarwal, P. Toliver, R. Menendez, T. Banwell, J. Jackel, and S. Etemad, "Spectrally efficient six-user coherent OCDMA system using reconfigurable integrated ring resonator circuits," *IEEE Photon. Technol. Lett.*, vol. 18, no. 18, pp. 1952–1954, Sep. 2006.
[66] J. P. Sokoloff, P. R. Prucnal, I. Glesk, and M. Kane, "A terahertz optical asymmetric demultiplexer (TOAD)," *IEEE Photon. Technol. Lett.*, vol. 5, no. 7, pp. 787–790, Jul. 1993.
[67] R. P. Scott, W. Cong, V. J. Hernandez, K. Li, B. H. Kolner, J. P. Heritage, and S. J. B. Yoo, "An eight-user, time-slotted SPECTS O-CDMA testbed: Demonstration and simulations," *J. Lightw. Technol.*, vol. 23, no. 10, pp. 3232–3240, Oct. 2005.
[68] Z. Zheng and A. M. Weiner, "Spectral phase correlation of coded femtosecond pulses by second-harmonic generation in thick nonlinear crystals," *Opt. Lett.*, vol. 25, pp. 984–986, 2000.
[69] W. Cong, C. Yang, R. P. Scott, V. J. Hernandez, N. K. Fontaine, B. H. Kolner, J. P. Heritage, and S. J. B. Yoo, "Demonstration of 160- and 320-Gb/s SPECTS O-CDMA network testbeds," *IEEE Photon. Technol. Lett.*, vol. 18, no. 15, pp. 1567–1569, Aug. 2006.
[70] W. Cong, C. Yang, R. P. Scott, V. J. Hernandez, N. K. Fontaine, J. P. Heritage, B. H. Kolner, and S. J. B. Yoo, "A sixteen-user time-slotted SPECTS O-CDMA network testbed," presented at the Opt. Fiber Commun. Conf., Anaheim, CA, 2006.
[71] R. P. Scott, W. Cong, C. Yang, V. J. Hernandez, J. P. Heritage, B. H. Kolner, and S. J. B. Yoo, "Error-free, 12-user, 10-Gb/s/user O-CDMA network testbed without FEC," *IEE Electron. Lett.*, vol. 41, pp. 1392–1394, Dec. 2005.
[72] V. J. Hernandez, W. Cong, J. Hu, C. Yang, N. K. Fontaine, R. P. Scott, Z. Ding, B. H. Kolner, J. P. Heritage, and S. J. B. Yoo, "A 320-Gb/s capacity (32-user × 10 Gb/s) SPECTS O-CDMA network testbed with enhanced spectral efficiency through forward error correction," *J. Lightw. Technol.*, vol. 25, no. 1, pp. 79–86, Jan. 2007.
[73] X. Wang, N. Wada, G. Cincotti, T. Miyazaki, and K. Kitayama, "Demonstration of over 128-Gb/s-capacity (12-User × 10.71-Gb/s/user) asynchronous OCDMA using FEC and AWG-based multiport optical encoder/decoders," *IEEE Photon. Technol. Lett.*, vol. 18, no. 15, pp. 1603–1605, Aug. 2006.
[74] T. H. Shake, "Security performance of optical CDMA against eavesdropping," *J. Lightw. Technol.*, vol. 23, no. 2, pp. 655–670, Feb. 2005.
[75] T. H. Shake, "Confidentiality performance of spectral-phase-encoded optical CDMA," *J. Lightw. Technol.*, vol. 23, no. 4, pp. 1652–1663, Apr. 2005.
[76] D. E. Leaird, Z. Jiang, and A. M. Weiner, "Experimental investigation of security issues in OCDMA: A code-switching scheme," *Electron. Lett.*, vol. 41, pp. 817–818, 2005.
[77] Z. Jiang, D. E. Leaird, and A. M. Weiner, "Experimental investigation of security issues in O-CDMA," *J. Lightw. Technol.*, vol. 24, no. 11, pp. 4228–4234, Nov. 2006.
[78] B. B. Wu and E. E. Narimanov, "A method for secure communications over a public fiber-optical network," *Opt. Express*, vol. 14, pp. 3738–3751, 2006.
[79] K.-i. Kitayama, "Code division multiplexing lightwave networks based upon optical code conversion," *IEEE J. Sel. Areas Commun.*, vol. 16, no. 7, pp. 1309–1319, Sep. 1998.
[80] Z. Jiang, D. S. Seo, D. E. Leaird, R. V. Roussev, C. Langrock, M. M. Fejer, and A. M. Weiner, "Reconfigurable all-optical code translation in spectrally phase-coded O-CDMA," *J. Lightw. Technol.*, vol. 23, no. 6, pp. 1979–1990, Jun. 2005.
[81] R. C. Menendez, P. Toliver, S. Galli, A. Agarwal, T. Banwell, J. Jackel, J. Young, and S. Etemad, "Network applications of cascaded passive code translation for WDM-compatible spectrally phase-encoded optical CDMA," *J. Lightw. Technol.*, vol. 23, no. 10, pp. 3219–3231, Oct. 2005.
[82] V. J. Hernandez, R. P. Scott, N. K. Fontaine, F. M. Soares, R. Broeke, K. Perry, G. Nowak, C. Yang, K. Okamoto, J. P. Heritage, B. H. Kolner, and S. J. B. Yoo, "SPECTS O-CDMA 80.8 km Bossnet field trial using a compact, fully integrated, AWG-based encoder/decoder," presented at the Opt. Fibers Conf., Anaheim, CA, 2007.
[83] J. P. Heritage, E. W. Chase, R. N. Thurston, and M. Stern, "A simple femtosecond optical third-order disperser," presented at the Conf. Lasers Electroopt., Baltimore, MD, 1991.
[84] N. K. Fontaine, C. Yang, R. P. Scott, V. J. Hernandez, K. Okamoto, D. L. Harris, J. P. Heritage, B. H. Kolner, and S. J. B. Yoo, "Security-enhanced SPECTS O-DCDMA demonstration across 150 km field fiber," presented at the Opt. Fibers Conf., Anaheim, CA, 2007.

Jonathan P. Heritage (S'74–M'75–SM'89–F'90) received the M.S. degree in physics from San Diego State University, San Diego, CA, in 1970, and the Ph.D. degree in engineering from the University of California, Berkeley, in 1975.

He was an Alexander von Humboldt Stiftung Postdoctoral Fellow at the Department of Physics, Technical University of Munich, Munich, Germany. From 1976 to 1984, he was with AT&T Bell Laboratories, Murray Hill, NJ. In 1984, he joined the newly formed Bell Communications Research, Red Bank, NJ, where he became a Distinguished Member of Professional Staff. Since 1991, he has been with the Department of Electrical and Computer Engineering, University of California, Davis, where he is currently a Professor of Electrical Engineering and Computer Science and Professor of Applied Science. He is the author or coauthor of more than 100 papers published in international journals. He is the holder of eight patents. His current research interests include optical microelectromechanical systems, optical code-division multiple access, and network issues, including device and link bit-error-rate modeling of wavelength-division-multiplexing networks.

Prof. Heritage is a Fellow of the Optical Society of America (OSA) and the American Physical Society. He was the corecipient (with A. M. Weiner) of the 1999 IEEE/Lasers & Electro-Optics Society (LEOS) W. J. Streifer Award for Scientific Achievement. He has been an Associate Editor of the IEEE JOURNAL OF QUANTUM ELECTRONICS and the IEEE PHOTONICS TECHNOLOGY LETTERS. He coedited the Special Issue on Ultrafast Optics and Electronics of the IEEE JOURNAL OF QUANTUM ELECTRONICS.

Andrew M. Weiner (S'84–M'84–SM'91–F'95) received the Sc.D. degree in electrical engineering from the Massachusetts Institute of Technology, Cambridge, in 1984.

Currently, he is the Scifres Distinguished Professor of Electrical and Computer Engineering in the Department of Electrical and Computer Engineering, Purdue University, West Lafayette, IN. From 1984 to 1992, he was with Bellcore, Morristown, NJ. He is the author or coauthor of more than 200 papers published in international journals and is the author of six book chapters. He is the holder of nine U.S. patents. His current research interests include ultrafast optics signal processing, high-speed optical communications, and ultrawideband wireless.

Prof. Weiner is a Fellow of the Optical Society of America. He was the recipient of numerous awards for his research. He has been a Co-Chair of the Conference on Lasers and Electro-Optics and the International Conference on Ultrafast Phenomena. He has also been a Secretary/Treasurer of IEEE Lasers and Electro-Optics Society (LEOS) and a Vice-President of the International Commission on Optics (ICO). He has served as an Associate Editor of several journals.